

Boletim Técnico da Escola Politécnica da USP

**Departamento de Engenharia de
Estruturas e Fundações**

ISSN 0103-9822

BT/PEF/9601

**Engineering Design of the Central
Core of the TBR - E Small Aspect
Ratio Tokamak**



Escola Politécnica - EPBC



31200053710

**R. M. O. Pauletti
R. M. O. Galvão
G. O. Ludwig
F. T. Degasperi
I. C. Nascimento**
São Paulo - 1996

905336

Engineering design of the central core of the TBR-E
small aspect ratio tokamak / R.M.O. Pauletti ...
[et al.]. -- São Paulo : EPUSP, 1996.
26p. -- (Boletim Técnico da Escola Politécnica da
USP. Departamento de Engenharia de Estruturas e
Fundações, BT/PEF/9601)

1. Reatores nucleares 2. Reatores de fusão ter-
monuclear I. Pauletti, Ruy Marcelo de Oliveira II.
Universidade de São Paulo. Escola Politécnica. De-
partamento de Engenharia de Estruturas e Fundações
III. Título V. Série.

CDU 621.039.4
621.039.62

Boletim Técnico da Escola Politécnica da USP

**Departamento de Engenharia de
Estruturas e Fundações**

ISSN 0103-9822

BT/PEF/9601

**Engineering Design of the Central
Core of the TBR - E Small Aspect
Ratio Tokamak**

**R. M. O. Pauletti
R. M. O. Galvão
G. O. Ludwig
F. T. Degasperi
I. C. Nascimento**

São Paulo - 1996

Engineering design of the central core of the TBR-E
small aspect ratio tokamak / R.M.O. Pauletti ...
[et al.]. -- São Paulo : EPUSP, 1996.
26p. -- (Boletim Técnico da Escola Politécnica da
USP. Departamento de Engenharia de Estruturas e
Fundações, BT/PEF/9601)

1. Reatores nucleares 2. Reatores de fusão ter-
monuclear I. Pauletti, Ruy Marcelo de Oliveira II.
Universidade de São Paulo. Escola Politécnica. De-
partamento de Engenharia de Estruturas e Fundações
III. Título V. Série.

CDU 621.039.4
621.039.62

ENGINEERING DESIGN OF THE CENTRAL CORE
OF THE TBR-E SMALL ASPECT RATIO TOKAMAK

R.M.O. Pauletti³, R.M.O. Galvão¹, G.O. Ludwig², F.T. Degasperi¹, I.C. Nascimento¹

¹Instituto de Física da Universidade de São Paulo
Laboratório de Física de Plasmas
C.P. 20516, CEP 01498, São Paulo, SP, Brazil

²Instituto Nacional de Pesquisas Espaciais

³Escola Politécnica da Universidade de São Paulo
e-mail: pauletti@if.usp.br

ABSTRACT

TBR-E is a small-aspect-ratio tokamak jointly proposed by the Institute of Physics of the University of São Paulo (USP), the Institute of Physics of the State University of Campinas (UNICAMP), and the National Institute for Space Research (INPE). The experiment is intended to investigate the spherical torus concept in conditions relevant to thermonuclear research, to develop new diagnostic techniques, and to explore new confinement regimes and current drive concepts.

The scientific program and basic design of the machine are described in another paper also presented to this workshop. The design of TBR-E brought up many novel engineering solutions, required to accommodate the inner legs of the TF coils (TFC), the main solenoid of the ohmic heating transformer (OHS) and the inner wall of the vacuum vessel in the very tight configuration of TBR-E, and yet to allow all of these components to be demountable.

Initially, this paper outlines the TBR-E TFC system, consisting of sixteen D-shaped coils. To increase coupling with the plasma loop, the inner legs of the toroidal field coils are placed inside the ohmic heating solenoid. Demountable joints between the outer TFC segments and the central straight segments are therefore required. The paper describes the technical solution for the problem of electrical connection between the inner and outer segments of the TFC as well as the use of these joints to provide the TFC system with a very compact and magnetically optimized scheme of symmetrical feeding buses.

The TBR-E OH solenoid (OHS) is discussed in the sequel. The OHS will be a two-layered, 220 turns, water cooled coil made of copper. A maximum current of 30 kA circulating in the coil will produce a maximum field of 7T. The paper outlines the geometry and electrical characteristics of the OHS. Of major concern for the design of central solenoids for tight aspect ratio tokamaks are mechanical and thermal stresses. The paper describes the accurate thermal analysis of the solenoid, considering the coupling of the temperature on both conductor and refrigeration fluid with the electrical potential and hydraulic pressure fields, and the mechanical stress estimates performed to assess the coil's safety.

THE TBR-E SMALL ASPECT RATIO TOKAMAK

TBR-E is designed to allow a continuous variation of the aspect ratio from 1.5 to 2.0, with fixed elongation and constant toroidal field, in order to characterize equilibrium, stability, and energy confinement as a function of the plasma aspect ratio. Because of its low aspect ratio, TBR-E will operate in the low collisionality regime even at rather low temperatures. Results obtained in TBR-E will thus extend the tokamak basis, in particular the confinement scaling, to low aspect ratio, in conditions physically equivalent to those achieved in large tokamaks.

A computer drawing of TBR-E is shown in Fig. 1. The overall dimensions, including the support structure, are 3.3 m high and 2.5 m wide. The major radius of the plasma column can be varied from 0.39 m to 0.50 m; the width of the plasma cross-section is approximately 0.25 m and the maximum elongation is 1.7; the maximum toroidal field at $R = 0.50$ m is $B_T = 0.63$ T. Finally, the maximum plasma current is $I_p = 240$ kA with approximately 80ms pulse duration. The basic constraint on the choice of parameters was the power available at the São Paulo Campus of USP, about 21 MW of peak power for short pulses. A rationale is given in [NASCIMENTO, 1991]. The device should cost around US\$ 6 millions, including power supplies but excluding diagnostic equipment. Detailed engineering design, construction, and assembly is expected to take four years.

The most crucial problems encountered in the engineering design of TBR-E relates to its tight configuration. Its low aspect ratio strongly affects the design of the innermost components, *i.e.*, the inner legs of toroidal field coils (TFC), the main ohmic heating solenoid (OHS), and the inner wall of the vacuum vessel (VV). The narrow space available to layout these components requires their integration to a high level. Altogether, they constitute what is usually called *the central core*. A frequent solution is to wind up the central solenoid directly over a cylinder made by the inner legs of the TFC (the central column, CC). With this choice, the connections between the CC and the outer segments of the TFC can be placed in a larger radius, and the need of a gap between the CC and the OH solenoid is avoided. However, fabrication is in this case more complicated than if the components were fabricated separately. Moreover, a hazard in one system, say the OHS, jeopardizes also the other (the TFC). For this reason, in TBR-E these systems have been designed such that they can be independently fabricated and assembled on site.

MAGNET SYSTEMS

A cross-section of TBR-E showing the major coil systems is shown in Fig. 2. The current will be driven by an air-core transformer (OHT). This includes the the ohmic heating solenoid (indicated in Fig. 2 by M1) and three pairs of compensating coils (M2, M3, M4) to decrease the flux leakage in the plasma region. Plasma equilibrium and shaping will be provided by a pair of vertical field coils (VFC) and two pairs of shaping and control coils (SFC1 and SFC2). All the above coils constitute the *poloidal field coil system*. The number and the position of all coils in this system have been chosen such as to avoid interference with diagnostic ports. The ohmic heating solenoid envelops the central column (CC), made by the inner legs of the toroidal field coils. To allow assembling and easy fabrication, the TFCs will have demountable joints between their outer segments and the central column.

TBR-E will normally operate with natural or slightly more elongated configurations. In this case, the vertical stability of the plasma column is not a severe problem and stabilization can be provided by a simple feedback system using

coils SFC1. For highly elongated configurations, an extra pair of radial field coils may be required. It has been recently verified that some plasma equilibrium configurations can be strongly perturbed by the stray field of coils M2 at the end of the current pulse.

TOROIDAL FIELD COILS SYSTEM

The toroidal magnetic field will be produced by 16 D-shaped copper coils connected in series. The maximum toroidal field on the equatorial plane at $R = 0.5$ m is $B_T = 0.63$ T for a current $I = 98.4$ kA flowing on the TFCs. The main parameters of the toroidal field coils are given in Table 1. The shape of the outer TFC segments minimizes bending stresses produced by the coils self-field, thus allowing a small cross-section to be employed. A study was made to select the most appropriate shape, considering the low aspect ratio requirements, as well as enough clearance to diagnostics in the outer side of the machine, and a total coil height not greater than 2.40 m. The parameters of the free-bending shape curve adopted are $R_1 = 0.07$ m and $R_2 = 1.12$ m. The material of the TFC will be OFHC copper in full hard conditions. The outer segments will be made up from straight bars, with square cross-section 45 mm x 45 mm, bent to the appropriate D shape in a calender machine. The straight, wedged shaped inner sectors will be made by extrusion, with cooling holes obtained during extrusion or lately, by drilling. The 16 inner sectors, bonded together but electrically insulated by glass-reinforced epoxy layers, 1 mm thick, constitute the central column (CC).

THE TFC ELECTRICAL CONNECTIONS

Joints between the central column and the outer segments of the TFC are critical in low aspect ratio tokamaks. From one hand, a small radius for the CC means a small amount of material to resist to electromagnetic loads that are proportionally higher than in conventional tokamaks, as they grow with the inverse of the distance to the machine axis. In TBR-E conditions are even worse, because the machine is designed to allow variable aspect ratio plasmas with constant toroidal field. Thus, the larger the aspect ratio of a discharge, the higher will be the required electrical current and so the electromagnetic loads.

- The TFC Crowns

For these reasons, a conventional bolted connection between the central column and the TFC outer segments was discarded. Instead, a *socket joint* was designed to ensure *mechanical continuity*, while *electrical connection* will be provided by *butt joints*, as shown in Fig. 3. Strips of *felt-metal* between the joining parts are used to decrease contact resistance. The required contact pressure has been experimentally determined for a sample of felt metal at room temperature. Fig. 4 shows the contact resistivity of a butt joint with a thin strip of felt metal as a function of the contact pressure. To achieve the pressure of 2 MPa required to keep the contact resistivity below $15 \mu\Omega\text{cm}^2$, a chain with 8 small hydraulic jacks surrounding the butt joints was devised. The chain compresses all the 16 joints against the central column, with a load of about 5 tons in each jack.

To facilitate assembling, *lap joints* were introduced at top and bottom positions of the TFCs. The short pieces between these joints and the butt joints with the central column (named the TFC "*crowns*") will be machined from copper plates. The electrical connection between coils will also be at the position of the lap joints.

- The symmetrical feeding buses

The current will be transferred from one TFC to another through two feeding buses, as shown in Fig. 5. This novel solution offers minimum increase to the total resistance of the circuit as well as reduction of fabrication and assembling costs.

Each bus will be composed by a series of machined copper pieces, imbricated one to another, in order to complete a ring. Each bus will also have a compensation ring, provided to balance the net toroidal current flowing in the bus. Half of the coils will be fed by one bus and half by another. This guarantees the symmetry and correct curvature of the error field produced by the residual toroidal current, in the plasma region, as shown in Fig. 6. Furthermore, a large region is obtained with error field smaller than 0.15 G.

A sketch of the current flow between the coils is shown in Fig. 7(a,b). A "pipeline" representation of the electrical flow is given in Fig 7(c). The current will enter the circuit by the lower bus and feed the eight even numbered coils. Then, using one of the coils' sectors, the current will be transferred to the upper bus, feed the eight odd coils, circulate through the compensation ring in the opposite direction, return to the lower bus, and after compensating the net current in the lower bus, finally leave the circuit.

THE TFC STRUCTURAL BEHAVIOR

The TBR-E geometry is conditioned mainly by the geometry of the toroidal field coils (TFC). Free-bending, D-shaped coils allow considerable material and manufacturing savings, as well as simplification of the geometry of the joints between the inner and outer sectors of each coil. On the other hand, as the machine aspect ratio is reduced, free-bending curves become "taller" and the central column gets thinner than in conventional tokamaks, complicating the design of the support structures for the toroidal and poloidal field coils.

- The inner central column mandrels

The outer sector of each TFC imposes to the ends of the central column a vertical load of about 2.4 tons, transferred through the socket connection between the outer segments of the TFCs and the CC. There arises a moment in the wedged sectors of the central column, due to the eccentricity between load and reaction. Although the copper wedges confine each other, they are separated by a softer epoxy layer. Thus the end of each wedge tends to bend inwards, producing high bending stresses in the reduced cross section of the socket region. Moreover, compressive hoop stresses could damage the insulating material. To avoid excessive bending stresses in the copper, or compression in the insulation, a mandrel-type prop will be inserted at each end of the CC. After the machine is assembled, a low intensity electrical current circulating in the TF circuit will heat the CC until it reaches the design temperature (81°C), when the mandrel is expanded. When the CC cools down, the mandrel will be compressing its inner face. To avoid damage to the insulation layer, an external clamp will compress the CC ends. On doing so, the ends of the CC will remain permanently in a state of compressive hoop stresses.

- The support structure

Because the TFCs are rather tall, it was necessary to support them against the out-of-plane forces (due to the interaction of the current in the TFC with the poloidal fields), in four distinct regions, both to prevent excessive lateral bending of the outer segments of the coils as to avoid excessive torsion of the central column (CC).

The TFC support structure will be made of two rings and two cylindrical caps (made from a fiber glass reinforced resin), interlocked by stainless steel bars, as shown in Fig. 8. In rings and cylindrical caps will be symmetrically placed with respect to the machine equatorial plane. Each ring will be divided into four quadrant segments, connected by bolts. The support structure will conveniently balance all electromagnetic loads due to normal and abnormal operational conditions, as well as transfer the weight of the components to the ground. On the other hand, the structure will not resist the thermal expansion of the coils and vacuum vessel, thus avoiding undesirable thermal stresses to take place.

The lateral loads on the TFC will be transferred to the rings by supports that avoid the lateral displacement of the coils, without restricting their thermal expansion. These supports, shown in Fig. 9, also transfer to the rings the loads acting on the vertical field coils and on the arms that support the VV and the shaping coils.

The out-of-plane loads due to the interaction between the TF currents and symmetrical poloidal fields are anti-symmetric with respect to the machine equator. Their resultant is null, but vertical torques appear in each ring or cap. These torques will be counterbalanced by the torques on the opposite ring or cap, through the *anti-torque frame*, with its rods alternately in axial tension and compression.

Besides balancing the torque in the vertical direction, this frame has two other functions: (1) it transfers the weight of the components to the lower ring, and from this to the ground and (2) it reacts to half the vertical load imposed by the outer segments of the TFC to the central column (40 ton), by means of a hydraulic jack placed inside the upper cap. Rigid stoppers compressing the CC were discarded because they would introduce undesirable thermal stresses both in the central column and in the support structure. The load of the hydraulic jack will be applied to the upper TFC crown by a stiff disk. By its turn, the lower crown will lay in another disk, that transfer the hydraulic load and the weight of the central column to the lower cap, through a rigid stopper (instead of another hydraulic jacket). An implication of this asymmetry is that the thermal expansion of the CC will be totally upwards.

The disks will be employed also to react to the lateral electromagnetic loads on the TFCs. For this propose, the disks will be connected to the caps by thin plates that oppose their rotations, still offering very little resistance to their vertical displacement, thus allowing the central column to breathe. Additionally to the connections through the disks, the caps will be connected to the feeding busses of the TF coils by means of bolts (Fig. 5). An elastomer layer is provided between the feeding bus and the cap. Together, these connections avoid excessive lateral displacements of the TFC coils and twisting of the central column without restricting the vertical thermal expansion of the coils.

Due to the torque produced by the out-of-plane loads on the TF coils, there is a maximum load of 2.3 ton on the rods of the locking frame, and a maximum load of 3.9 ton on the rods of the principal frame. The vertical hydraulic system adds a tension of 4.2 ton on the rods of the locking frame and 3.7 ton on those of the principal frame.

Because of the low bending stiffness of the TF coils, the PF coils and the vacuum vessel (VV) could not be supported directly from them. Convenient support arms have been required, to withstand the gravity and electromagnetic loads on the PFC and VV.

PRELIMINARY STRESS ANALYSIS OF THE TFC

Stress analyses of the TFC were developed with the aid of an in-house finite element code (ANLEF). Fig. 10(a) shows the mesh employed. The in-plane loads (due to the self-field of the coil) are symmetrical with respect to the machine equator, while the out-of plane loads are either anti-symmetrical (in the case of normal and most of the abnormal poloidal field configurations), or symmetrical (in the case of fault conditions, characterized by a short-circuit in one TFC). Therefore, only one half of the coil was modeled, with convenient boundary conditions to represent symmetry or anti-symmetry. In the central column region, the TFC confine each other, thus an equivalent radial stiffness was simulated using spring elements.

- In-plane loads

Fig. 10(b) shows the resulting displacement in the TFC under the in-plane loads. Both displacements and the constant tension of 22 kN resulting along the outer sector of the coil agree well with the values predicted analytically. In the central column, the tension increases to 24 kN, due to the additional vertical load in the region of the joint. The end of the CC undergoes a vertical displacement of 0.27 mm which introduces some bending along the development of the coil. The bending moment is maximum at the end of the central column, due to the axial eccentricity between of crown and central column. The model did not consider the vertical compression system and the inner mandrel prop described above, which have been designed lately, specifically to limit stresses in the weak region of the socket connection.

- Out-of-plane loads

Magnetic fields and forces for the different scenarios of the current flow in the PFC (corresponding to normal and abnormal operational conditions) were computed with the aid of an in-house program (BFORCE). Displacements, bending moments, internal shear and torsion moments have been obtained from ANLEF for all the different scenarios, showing the safety of the TFC under normal condition out-of-plane loads. On the other hand, loads due to fault conditions are usually one order of magnitude larger than operational loads. Stresses in this case may well exceed the safety limits, even though larger allowable stresses are assumed, taking into account the low number of fault events. To avoid the mechanical failure of the coils during a short circuit, it may be necessary to provide them with removable intermediate spacers, which reduce the lateral deformation of the coils. Loads under fault conditions will be considered during the detailed engineering design.

OHMIC HEATING SOLENOID

The OHS, shown in Fig. 10, is the main coil (M1) of the plasma current drive and heating system (the *magnetizing system*), which comprises also three pairs of compensating coils, M2, M3, M4, connected in series with the OHS to decrease the flux leakage in the plasma region (the resulting field configuration

and " $|B| = \text{constant}$ " curves for $I_{\text{OHS}} = 30 \text{ kA}$, are shown in Fig. 11). A high-order null is produced at the equatorial plane. The error field is smaller than 10 G inside an approximately circular contour of 10 cm radius centered at the position of the field null).

The major parameters of the magnetizing system are shown in Table 2. The system lumped circuit parameters are: resistance $R = 18 \text{ m}\Omega$ and inductance $L = 1.36 \text{ }\mu\text{H}$. The estimated mutual inductance with the plasma column, considered as a simple current loop located at the equatorial plane, at $R = 0.45 \text{ m}$, is $M \cong 6.5 \text{ }\mu\text{H}$. Coils M1 (the OH solenoid) and M2 are two layer solenoids and will be helically wound. Coil M3 has only two radial layers and will be bound together with the shaping coil SFC2. Coil M4 has only one turn and will be located underneath the edge of some flanges of the vacuum vessel. To fit it in place, this coil will be made in two separate arcs which will be bolted together, during assembly, in the final position. All compensation coils will be made from copper bars of $2 \times 2 \text{ cm}^2$ cross-section, including isolation. The maximum current density in these coils will be $j = 8.3 \text{ kA/cm}^2$ and preliminary thermal analyses indicate that they can be cooled between shots solely by natural air convection.

By its turn, the OHS will be made by the winding in two layers (a total of 220 turns) of copper conductor. The conductor will have rectangular cross-section ($A_s = 9 \times 15 \text{ mm}^2$), with a central cooling hole ($\phi = 4 \text{ mm}$). The coolant will be demineralized water. In order to minimize the thermal gradient in the radial direction, each layer of will be cooled by an independent hydraulic circuit. The inner and outer radius will be 7.3 and 10.5 cm, respectively. The conductor will be wrapped with a Kapton strip. After winding, the turns will be glued with an epoxy resin, giving a total insulation thickness (Kapton + epoxy) of 1 mm. The electrical feeds of the central solenoid will be embedded in an epoxy jacket placed around the central column, as indicated in Fig. 3. This will require that the vacuum vessel be assembled in place before the central solenoid, which is then slid in between the central column and the vessel. Because of the narrow gaps (2 mm) between the solenoid and the other components of the central core, the tolerances in the coil final dimensions are very restrictive.

THERMAL ANALYSIS OF THE OHMIC HEATING SOLENOID

The OHS will be charged to a maximum current of 30kA and then rapidly discharged on a load resistor to produce plasma breakdown and current ramp-up. Because of the small space available between the inner wall of the vacuum vessel and the central column, the current density in the OHS is very high at the peak of magnetizing current, arising concern about the coil safety.

Due to the short pulse duration, shown in Fig. 13, heating of the OHS is practically adiabatic. Then solenoid will be cooled during the idle time between pulses. Although simple zero dimensional evaluations can be carried out the thermal excursion of the OHS, information about the thermal gradients on the coil due to the cooling process and the time required to cool down the system was obtained with the more sophisticated model sketched in Fig. 14, considering the convective heat exchange between conductor and coolant, as well as the material non-linearities. Since the each layer has an independent circuit, only the external one (total length 67.1 m) is discretized. Results can be roughly extended to the inner layer, taking the first 58.1 meters of the model.

The model was studied with the aid of the ANSYS program. The conductor and the hydraulic circuit were discretized with, respectively, thermoelectric and thermohydraulic unidimensional elements, connected with convective links. The applied loads were: electrical current on the initial end of the conductor and electrical potential on the final end; flow velocity and temperature (20 °C, equal to the initial coil temperature) on the initial end of the hydraulic circuit and zero pressures on the final end. Fig. 15(a) shows the temperature evolution in the initial and final ends and at some equispaced points along the conductor, for a flow velocity of 4 m/s. The total time to cool down the solenoid is about 4 minutes. Fig. 15(b), which shows the same curves plotted against the logarithm of time, helps visualizing the temperature excursion during the current shot as well as the maximum temperature reached by the solenoid, 47 °C.

Shear stresses at the insulation, due to the differential expansion between turns, are critical for the safety of the central solenoid. Fig. 15(c) shows the evolution of the temperature difference between nodes 1 and 2 (worst case). The maximum difference is 9.1 °C, at $t = 3$ s. Assuming a linear variation between nodes, a maximum temperature difference of 4.1 °C between turns is obtained. An axisymmetric stress analysis showed that the shear stresses are below 5 MPa, an acceptable value. However, an excessive pressure (3.6 MPa) was required to sustain a flow velocity of 4 m/s. A new analysis was then developed, reducing the velocity to 2 m/s. The total cooling time then increased to 8 minutes while the inlet pressure dropped to 1.1 MPa. The maximum temperature difference between nodes 1 and 2, although delayed to 5.5 seconds, raised to 10.1 °C, still an acceptable value.

Safety of the OHS against the electromagnetic loads was also investigated. For the peak current flowing on the solenoid (30kA), there results an *average hoop stress* of 59.1 MPa. The *peak hoop stress* was evaluated with a thick pipe idealization, using Lamé's formula, to give 93.4 MPa. However, the OHS will be under a further compressive load in the vertical direction due to the mutual attraction force between the solenoid and the M2 coils. Assuming this load to be fully transferred by the jackets of the CC to the solenoid, the average compressive stress in the vertical direction amounts 6.9 MPa. For OFHC copper and for an expected life-time of $2 \cdot 10^5$ cycles and if one admits $\sigma \leq 150$ Mpa, a 50% safety margin is obtained for the calculated values — since $\max(\sigma_\theta - \sigma_v) = 100.3$ MPa — that accommodates possible dynamic magnifications of the stresses.

REFERENCES

- [NASCIMENTO, 1991] Nascimento, I.C., Galvão, R.M.O., Pauletti, R.M.O., Tuzel, A.G., Sá, W.P., Degasperi, F.T., Bignardi, F.R., Coelho-Nascimento, N., Elizondo, J.I., Caldas, I.B., Machida, M., Sakanaka, P.H., Ludwig, G.O., Montes, A., Ueda, M., Li, Y., Shi, J. *The TBR-E Project - Basic Engineering Design*. IFUSP/INPE/UNICAMP. São Paulo, 1991 - Relatório de Projeto.

Parameters	Values
Number of coils	16
Current (kA)	98.4
Turns per coil	1
Shape	D
Height (m)	2.4
Inner radius, R1 (m)	0.05
Outer radius, R2 (m)	1.12
Outer leg cross-section (cm^2)	4.5×4.5
Inner leg cross-section	22.5 arc; $2.5 \leq r \leq 6.8$ cm
Material	OFHC copper (full hard)
Resistance ($m\Omega$)	1.5
Inductance (mH)	0.309
Toroidal field on axis, R=0.5 m (T)	0.63
Adiabatic temperature rise; inner leg ($^{\circ}C$)	51
Pulse repetition rate	1 pulse each 5 minutes

Table 1 Main parameters of the Toroidal Field Coils System.

Parameters	Values
Inside radius, r_1 (cm)	7.3
Outside radius, r_2 (cm)	10.5
Length, l (cm)	110.0
Number of turns, N	220
Number of radial layers	2
Conductor cross-section area (cm^2)	1.5×0.9
Insulation thickness (cm)	0.1
Cooling hole diameter (cm)	0.5
Packing factor	0.72
Maximum current density (kA/cm^2)	26.0
Resistance at 20 °C ($m\Omega$)	15.8
Inductance (mH)	1.15
Central field (T)	7.5
Total flux swing (Wb)	0.38
Material	OFHC
Peak hoop stress (MPa)	100.3
Adiabatic temperature rise (°C)	83.5

Table 2 Main parameters of the ohmic heating solenoid.

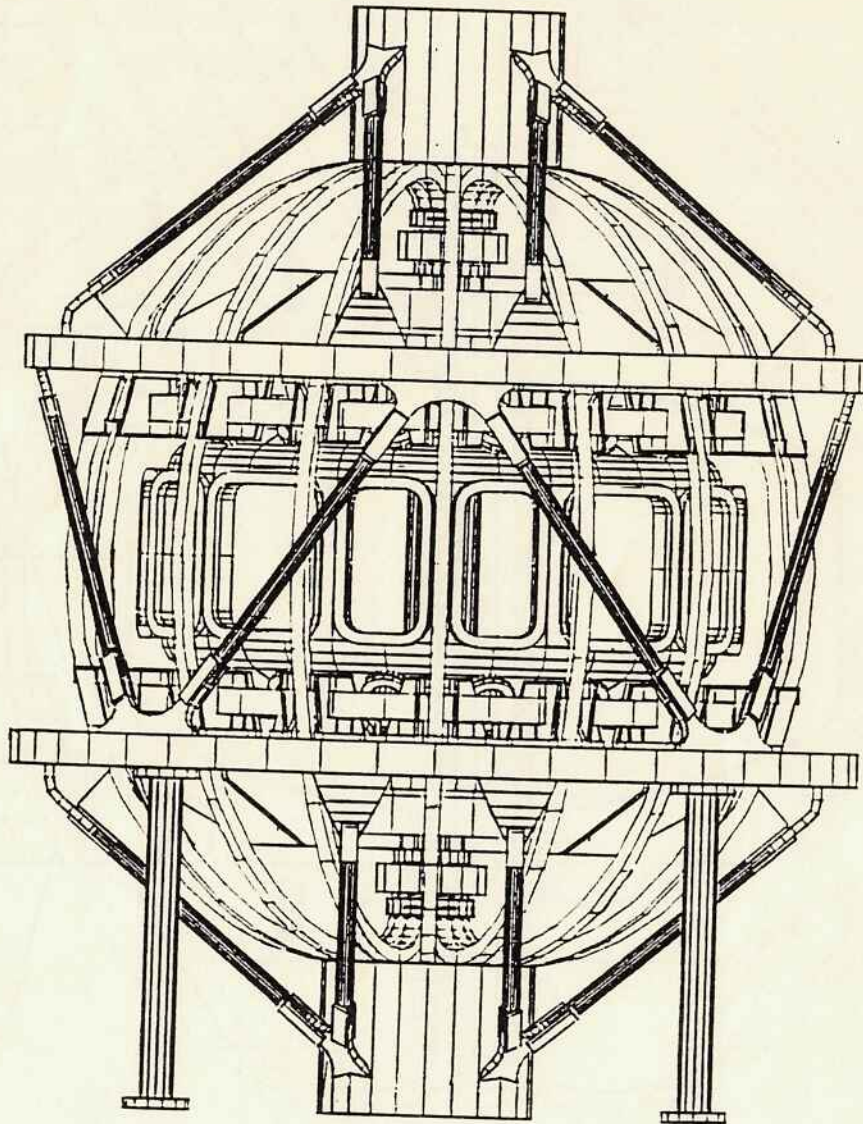


Figure 1 The TBR-E tokamak

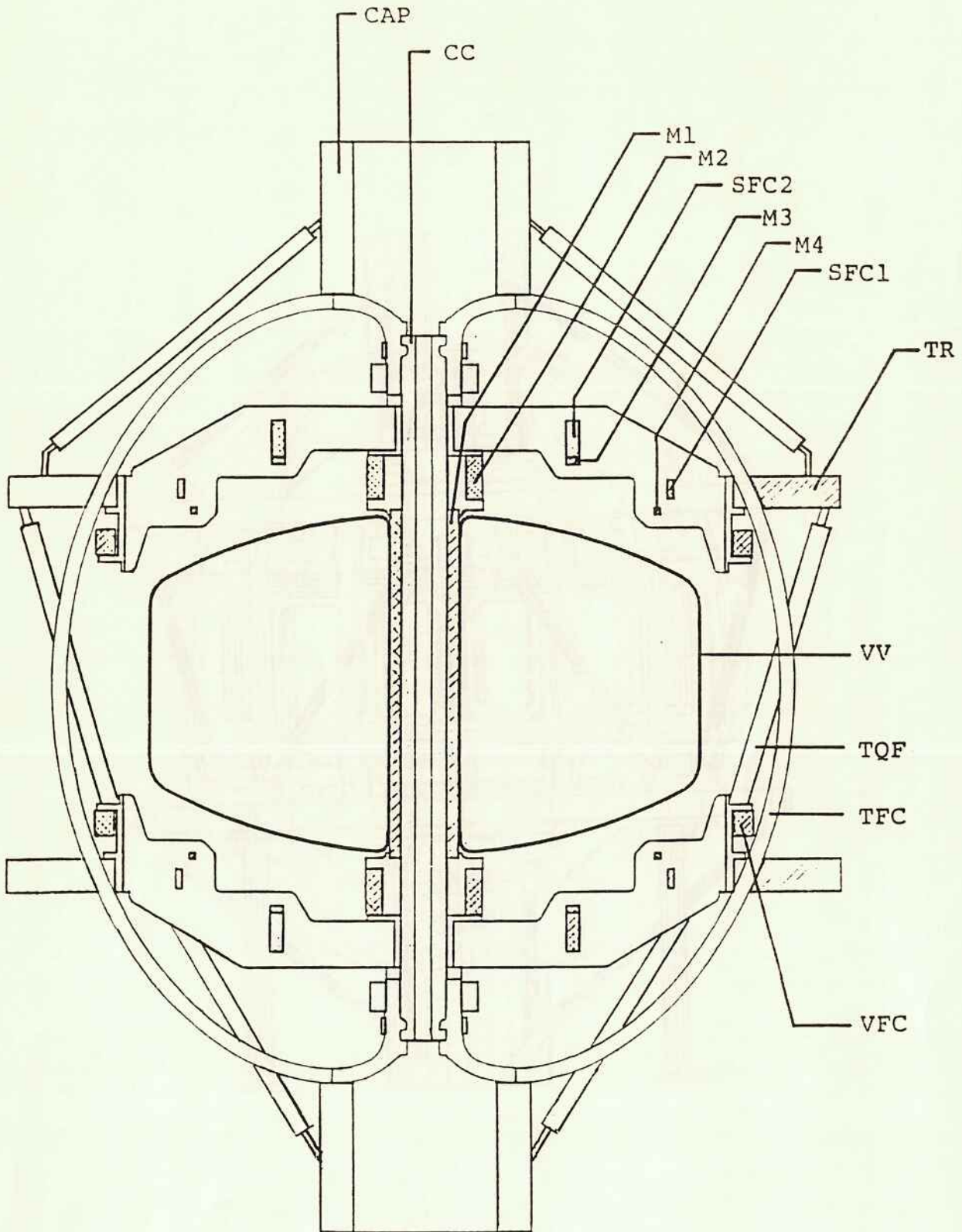


Figure 2 Cross-section of TBR-E showing the toroidal field coils (TFC), central column (CC), vacuum vessel (VV), magnetizing coils (M1-M4), vertical field coils (VFC), shaping coils (SFC1 and SFC2). Also shown is the support structure: toroidal rings (TR), caps, and torque frame (TQF).

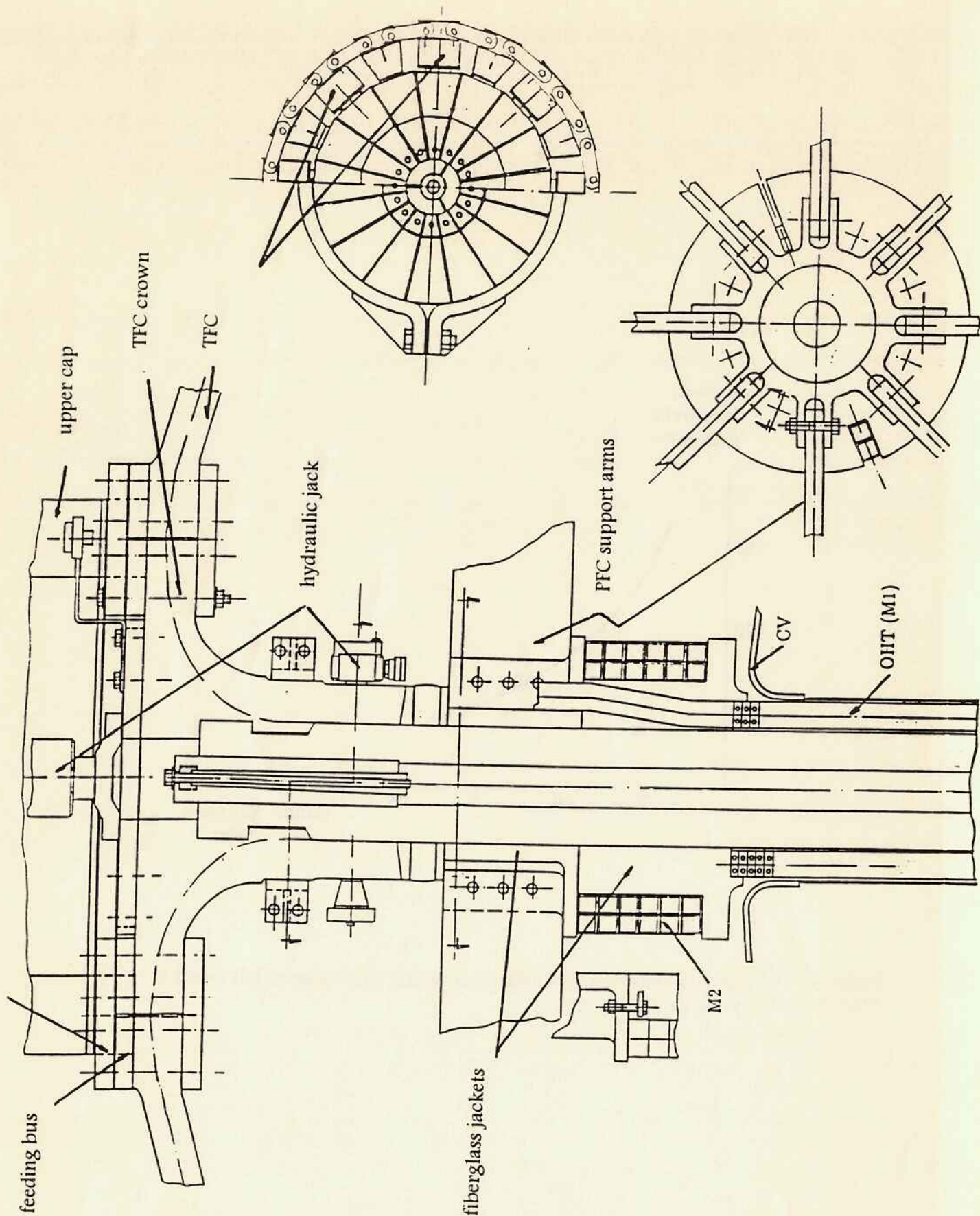


Figure 3 Arrangement of the central core of TBR-E, showing the ohmic heating solenoid M1, the compensating coil M2, the supporting arms of the poloidal field coils, the socket joint between the TFC crowns and the central column, and the hydraulic system employed to compress the ends of the central column.

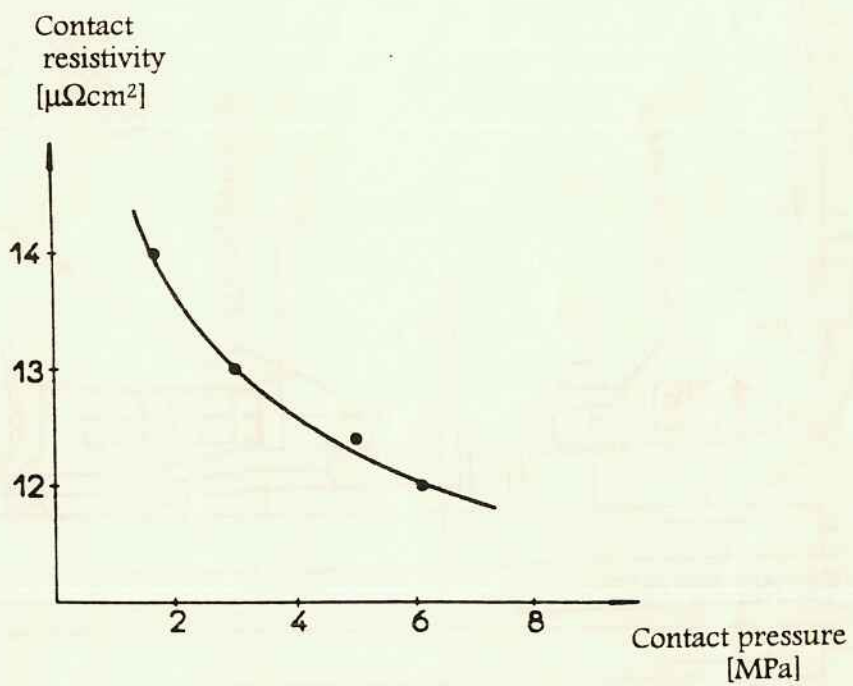


Figure 4 Contact resistivity of a butt joint with a thin layer of felt metal as a function of the pressure on the joint.

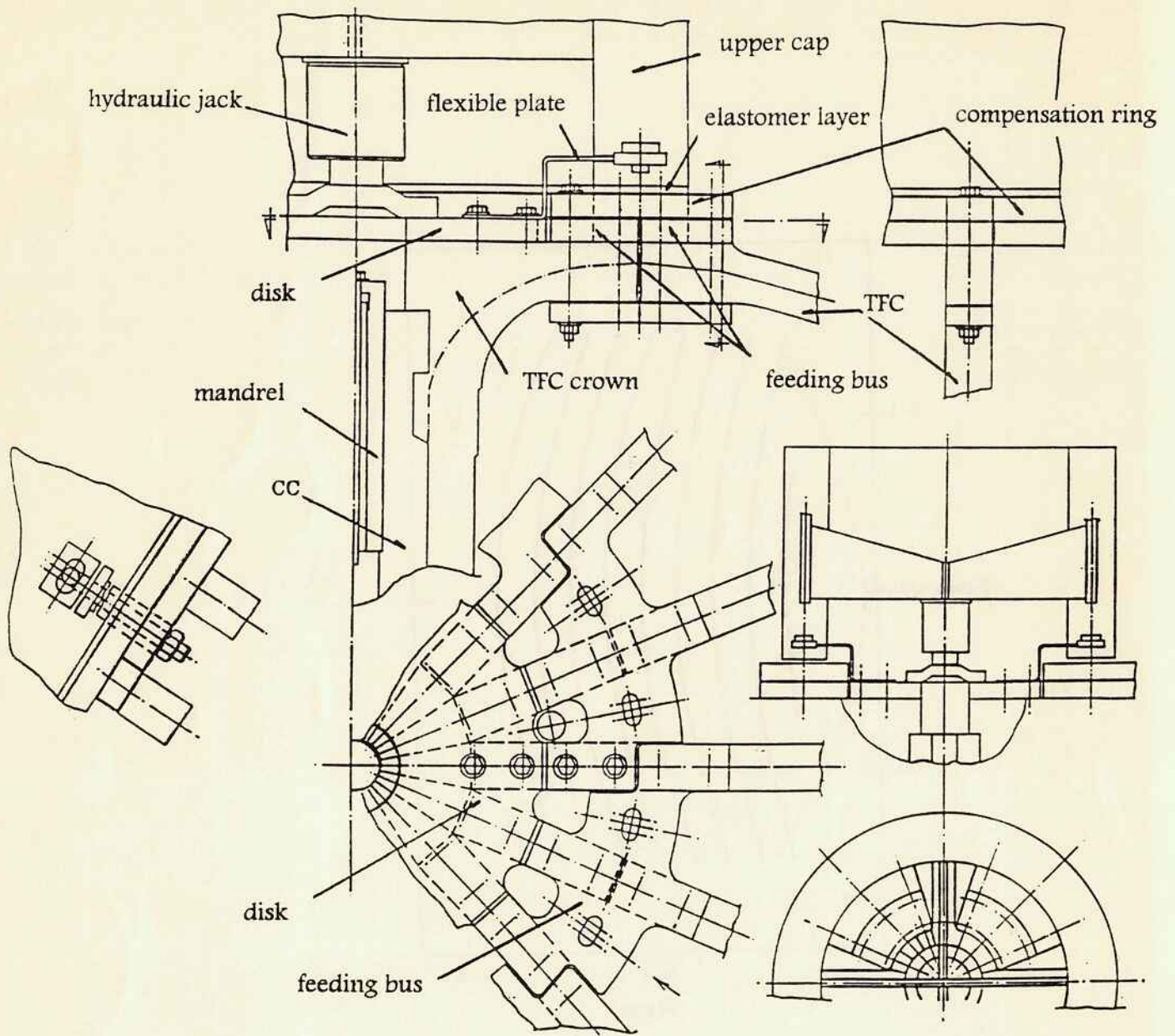


Figure 5 Detail of the TFC crowns and feeding bus.

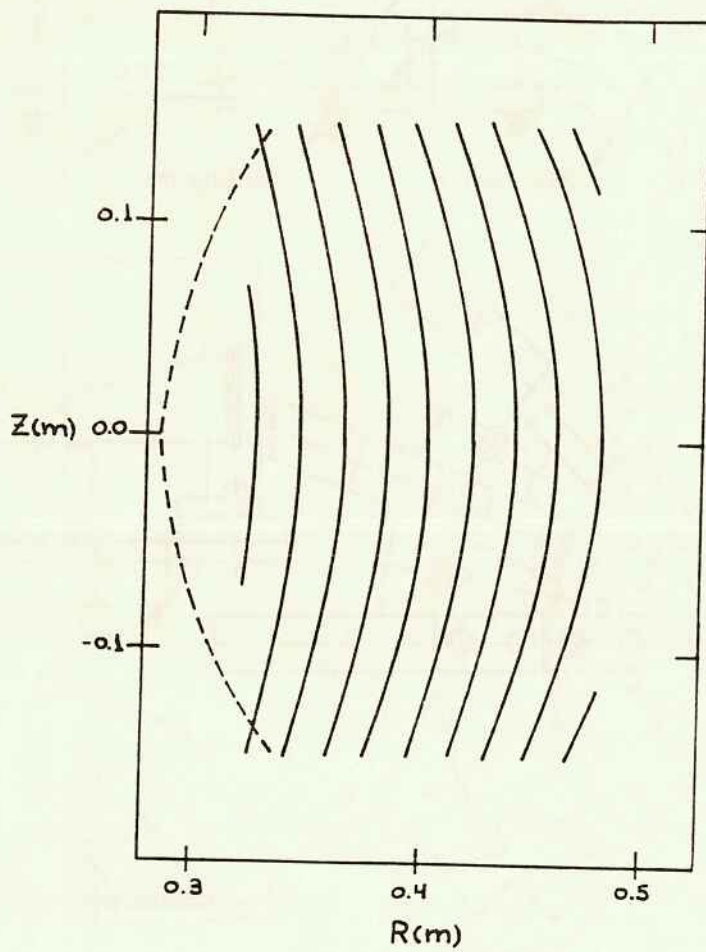


Figure 6 Field lines of the error field produced by the feeding buses of the toroidal field coils. The region to the right of the dashed line has an error field smaller than $1.5 \cdot 10^{-5}$ T for a current of 100 kA in the feeding buses.

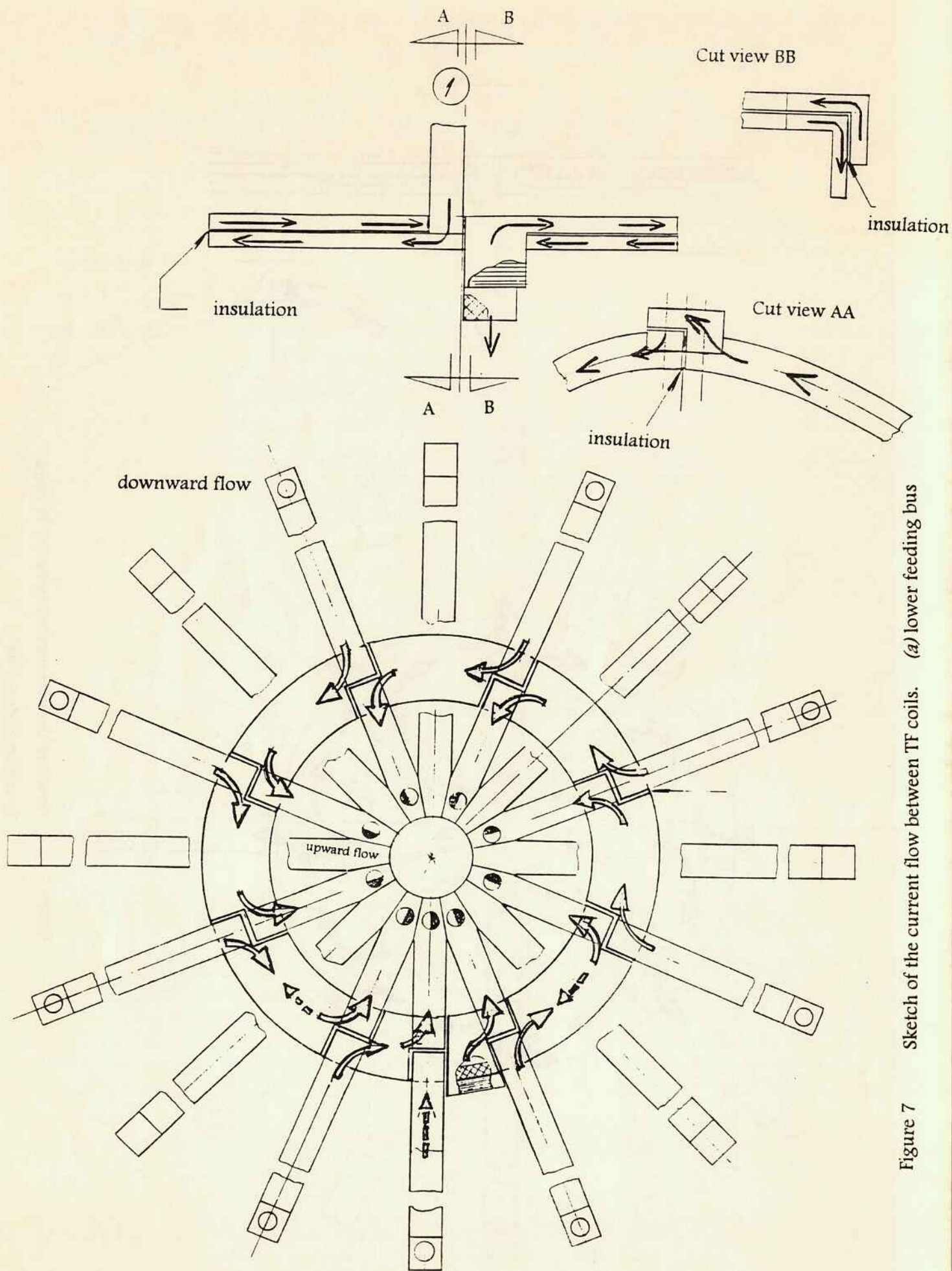


Figure 7 Sketch of the current flow between TF coils. (a) lower feeding bus

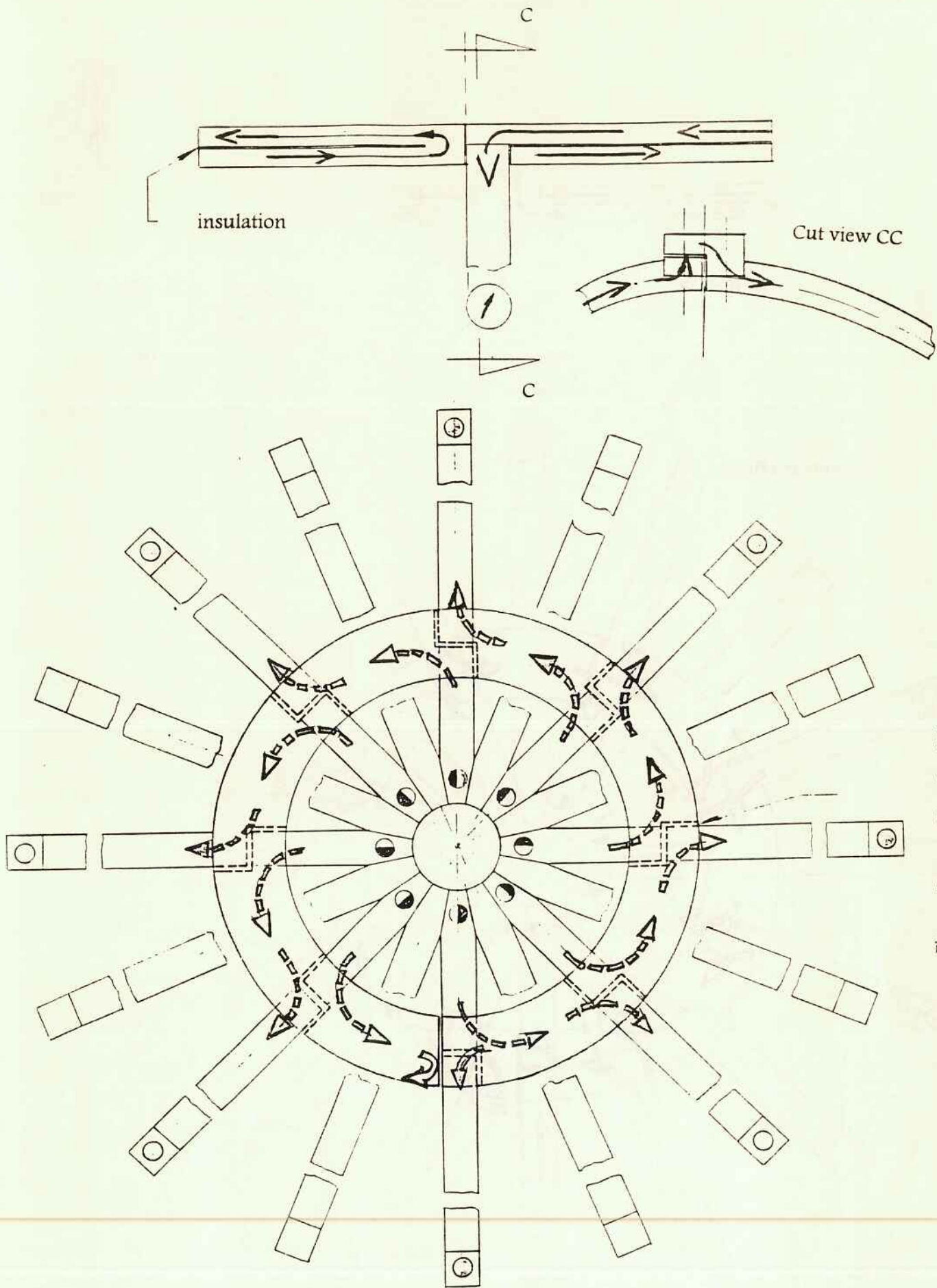


Figure 7 Sketch of the current flow between TF coils.
 (b) upper feeding bus

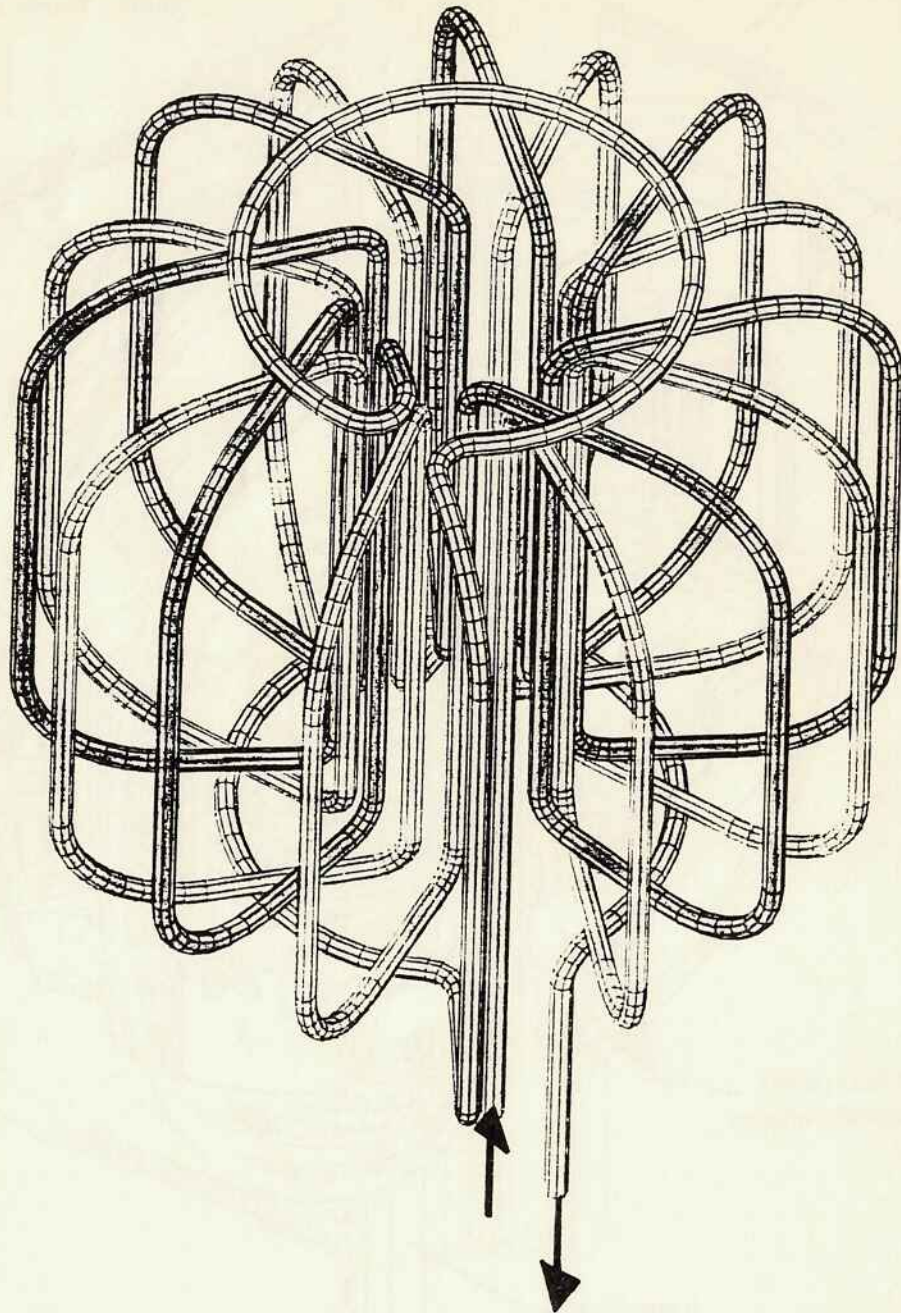


Figure 7

Sketch of the current flow between TF coils.

(c) pipeline representation of the electric flow in the TF coils

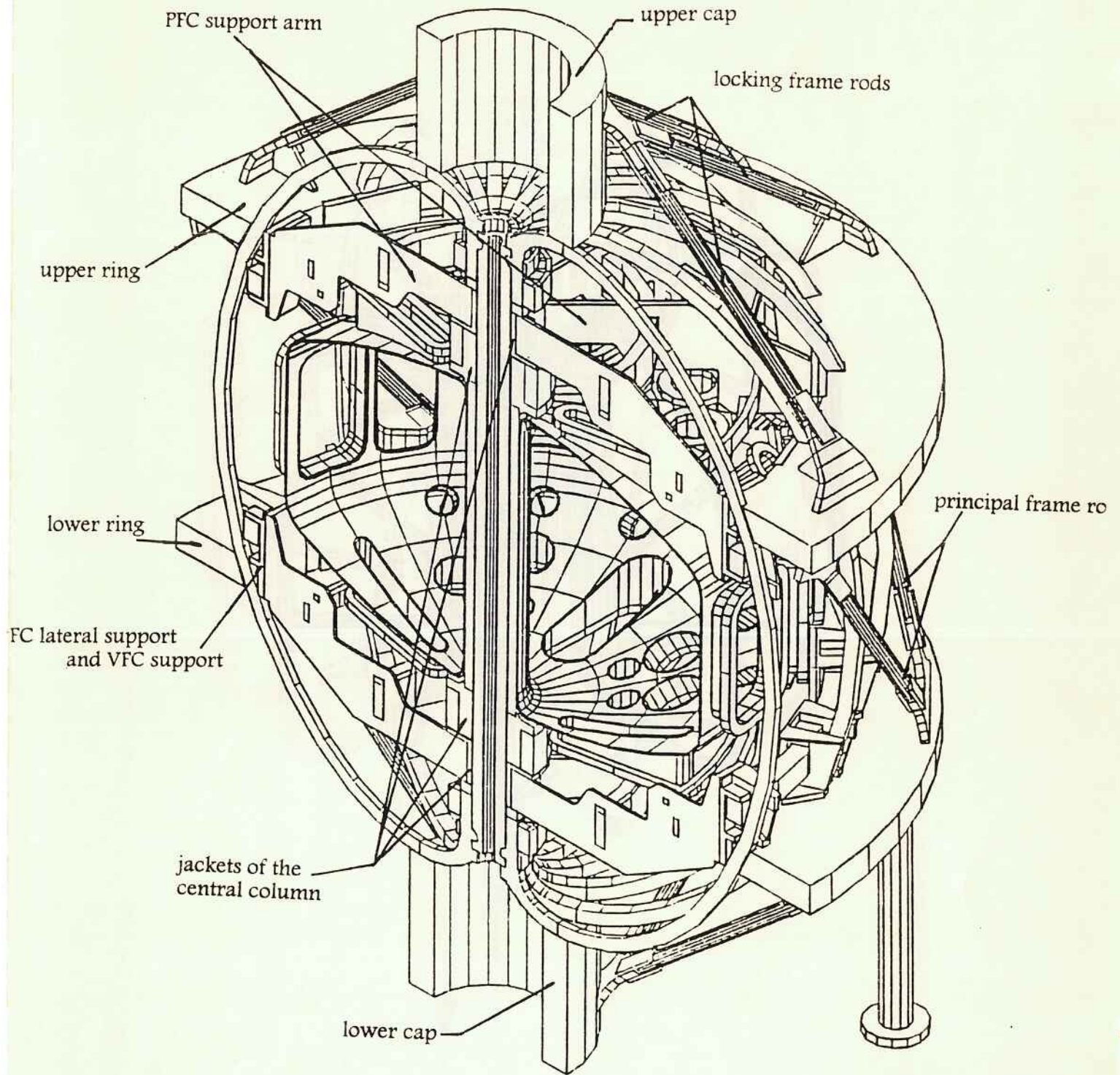


Figure 8 Main components of the support structure.

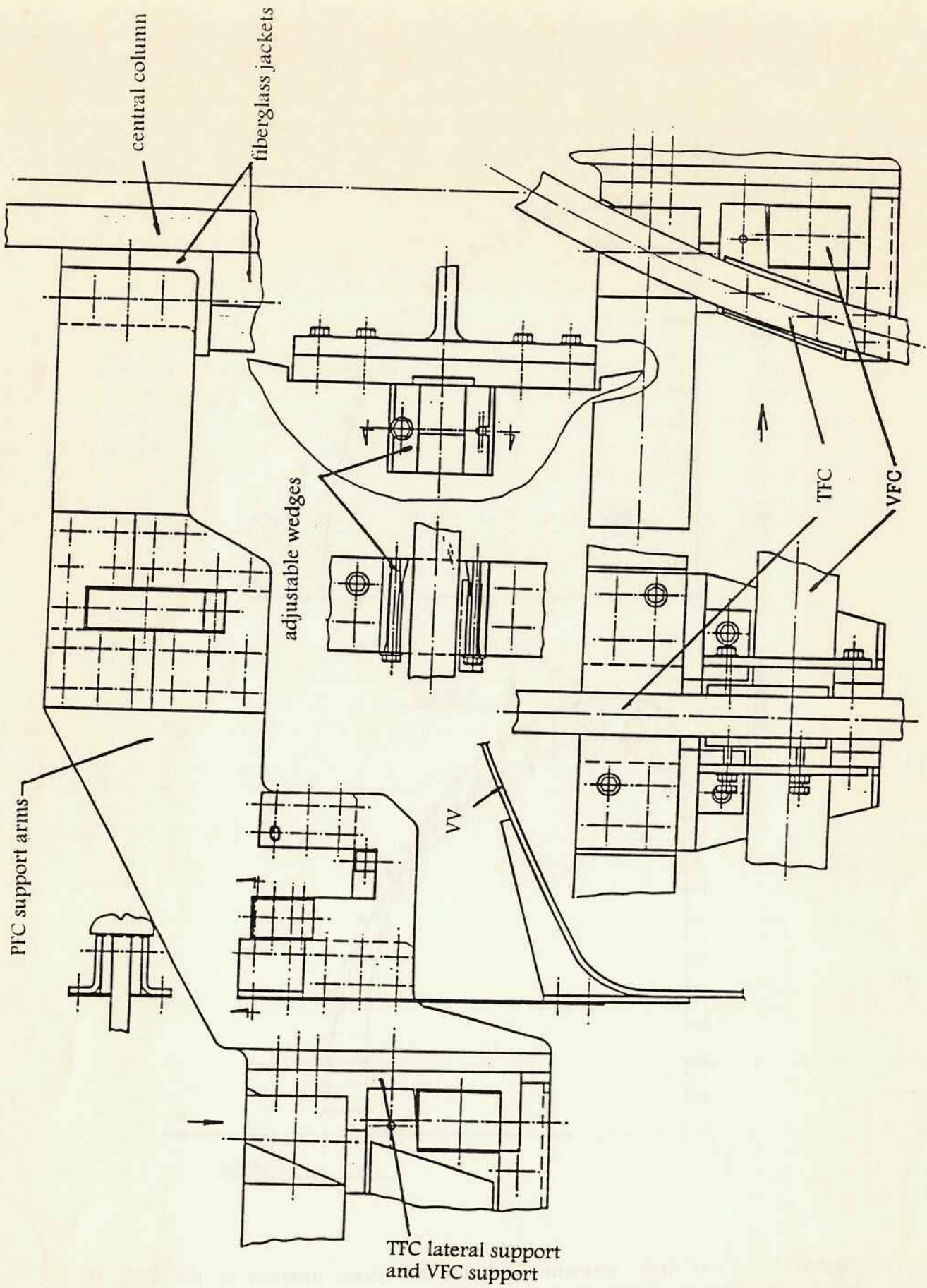


Figure 9 Supports of the poloidal field coils.

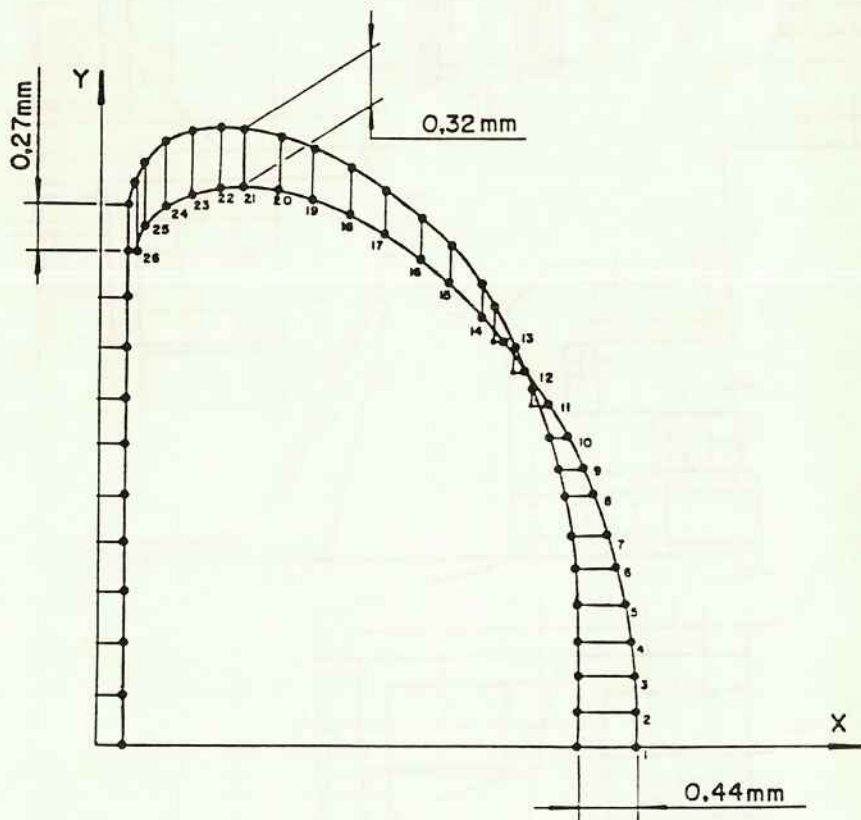
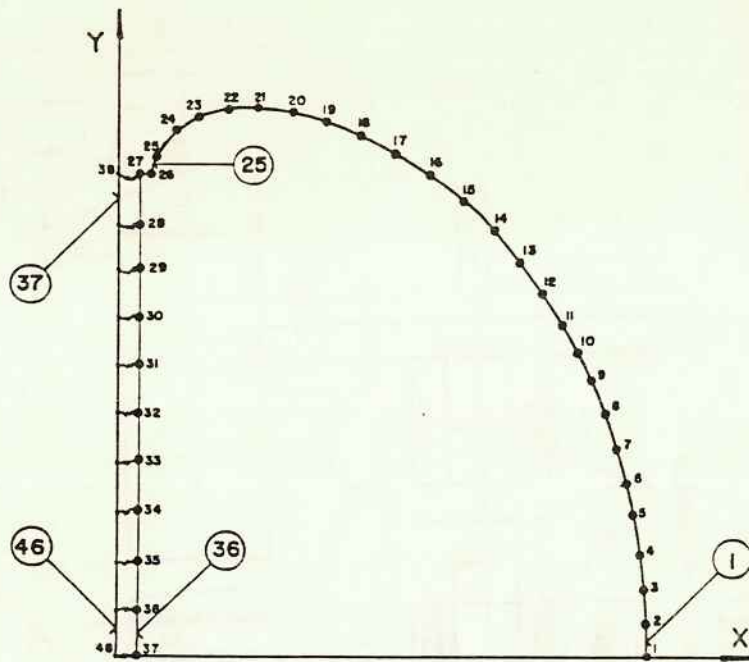


Figure 10 (a) finite element mesh for the stress analysis of the TFC; (b) displacements of the TFC under in-plane loads.

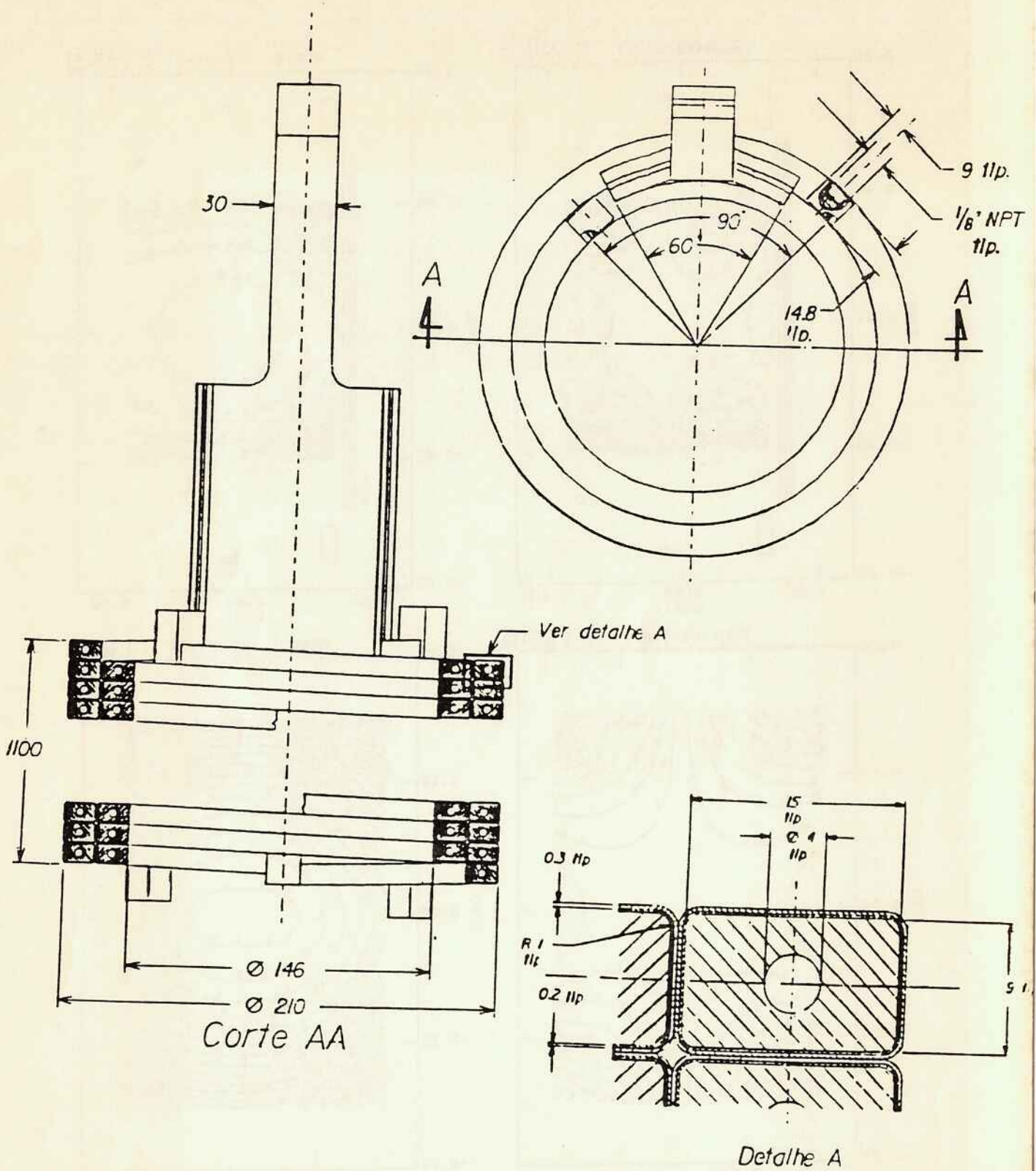


Figure 11 Ohmic heating solenoid (OHS).

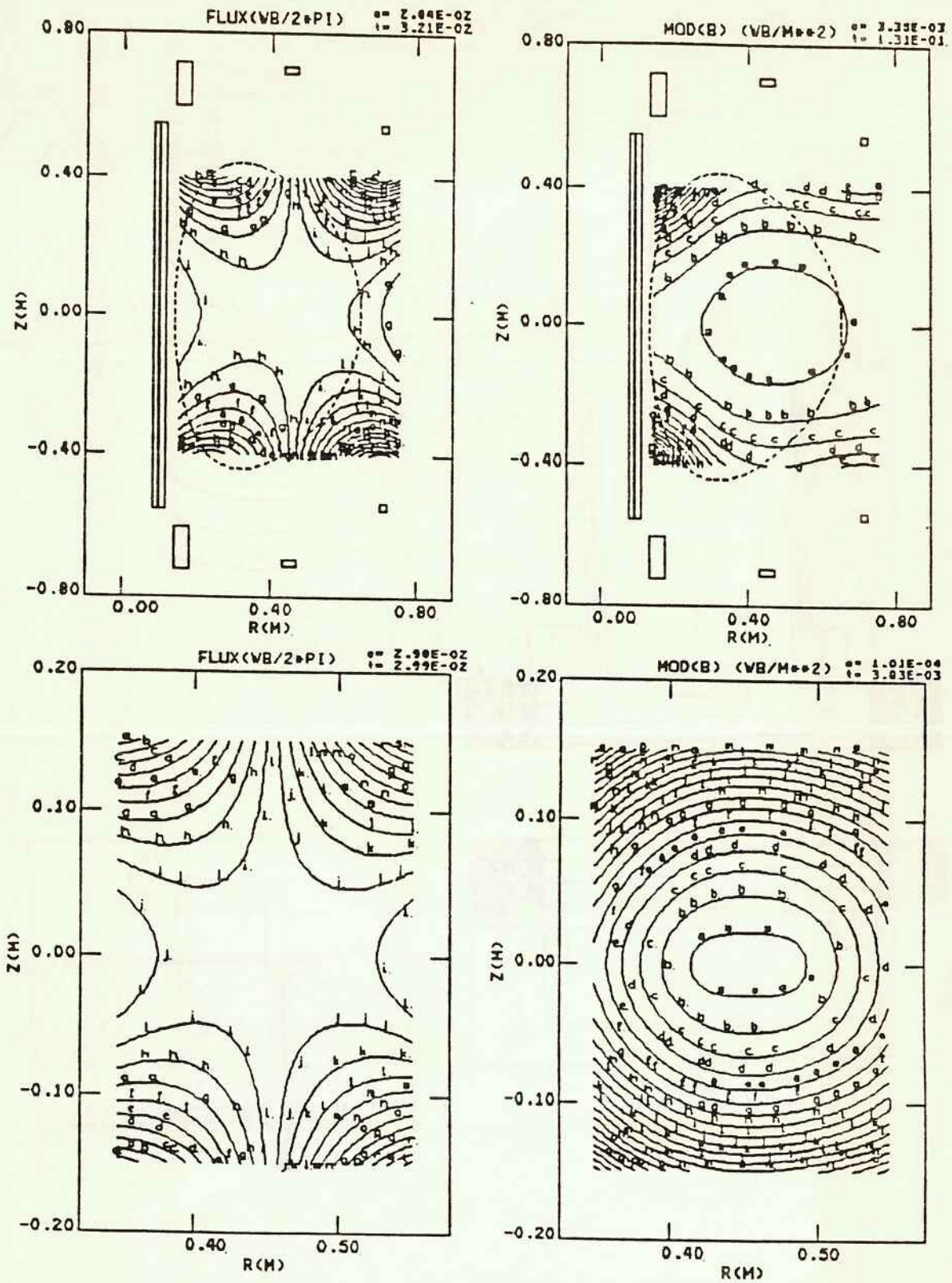


Figure 12 Field lines (a), (b) and $|B| = \text{constant}$ curves (c), (d), for a current $I=30$ kA in the magnetizing coils.

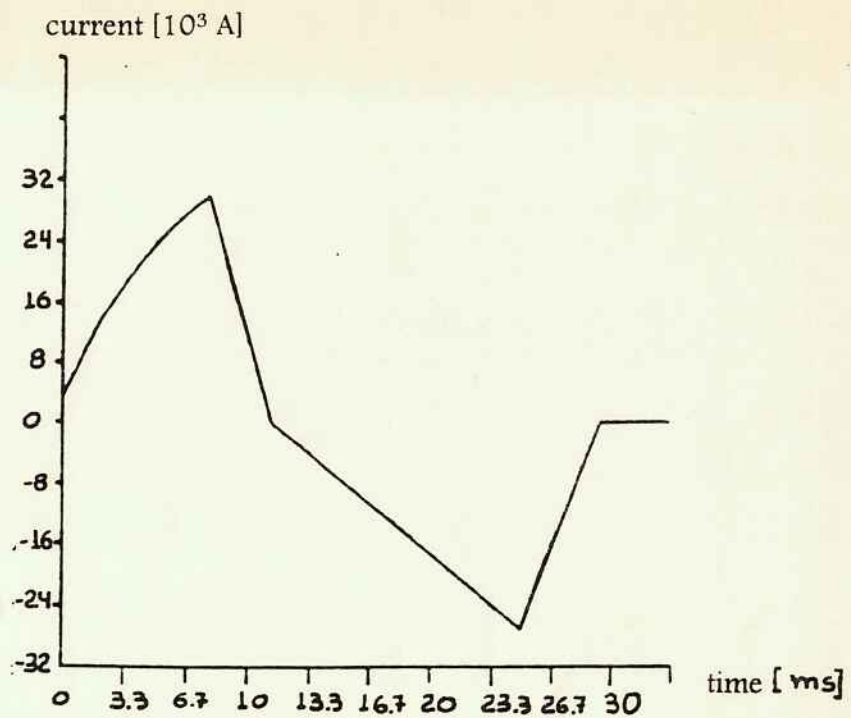


Figure 13 Current pulse applied to the ohmic heating solenoid.

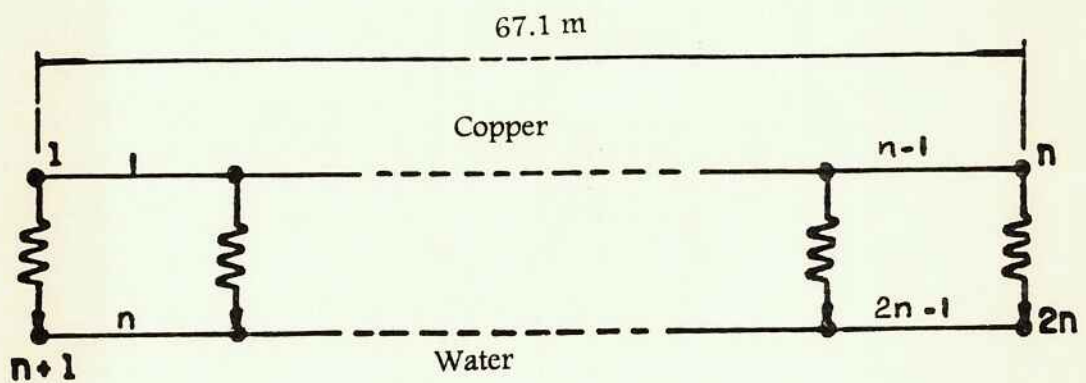
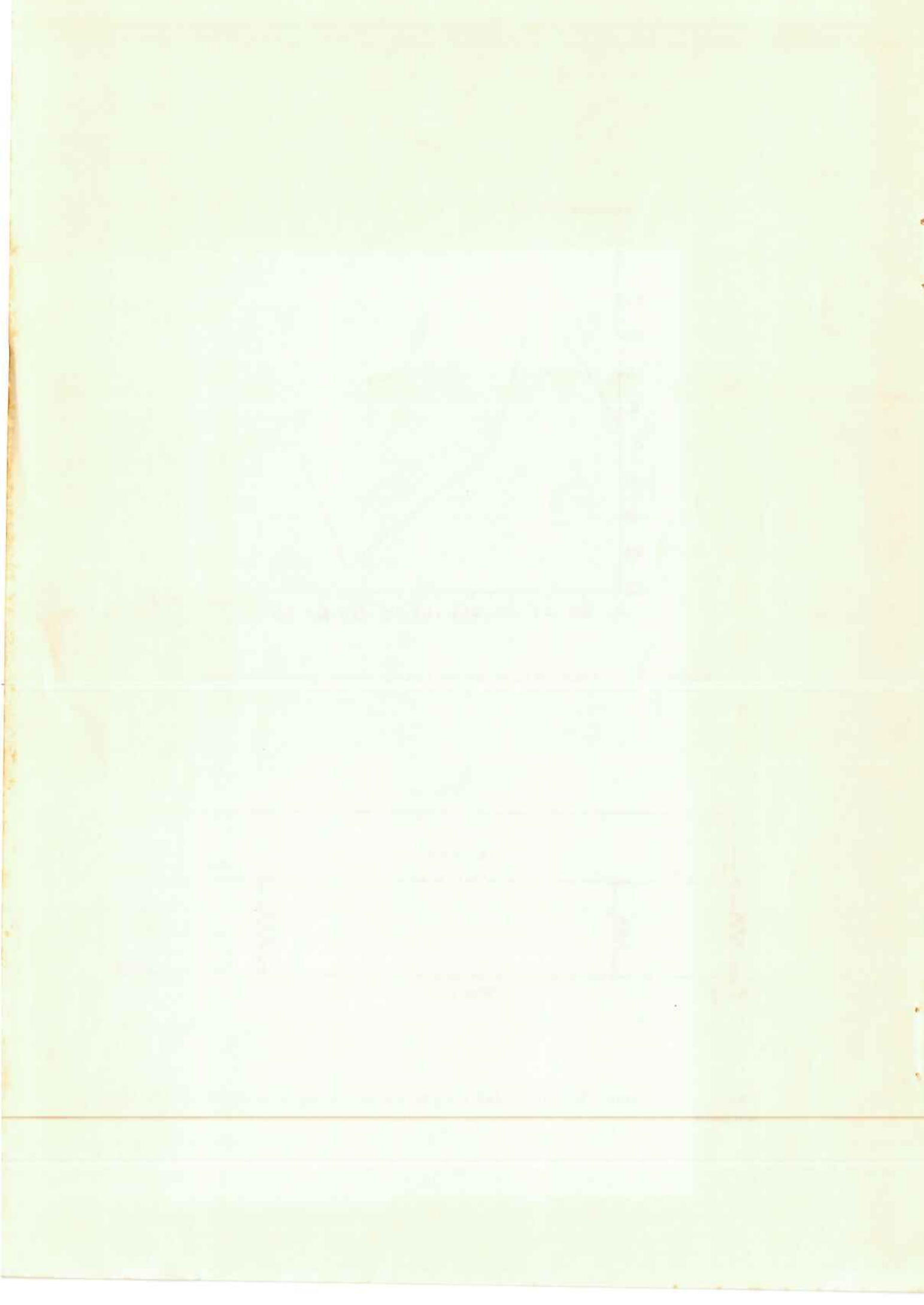


Figure 14 Finite element model for the thermal analysis of the ohmic heating solenoid.



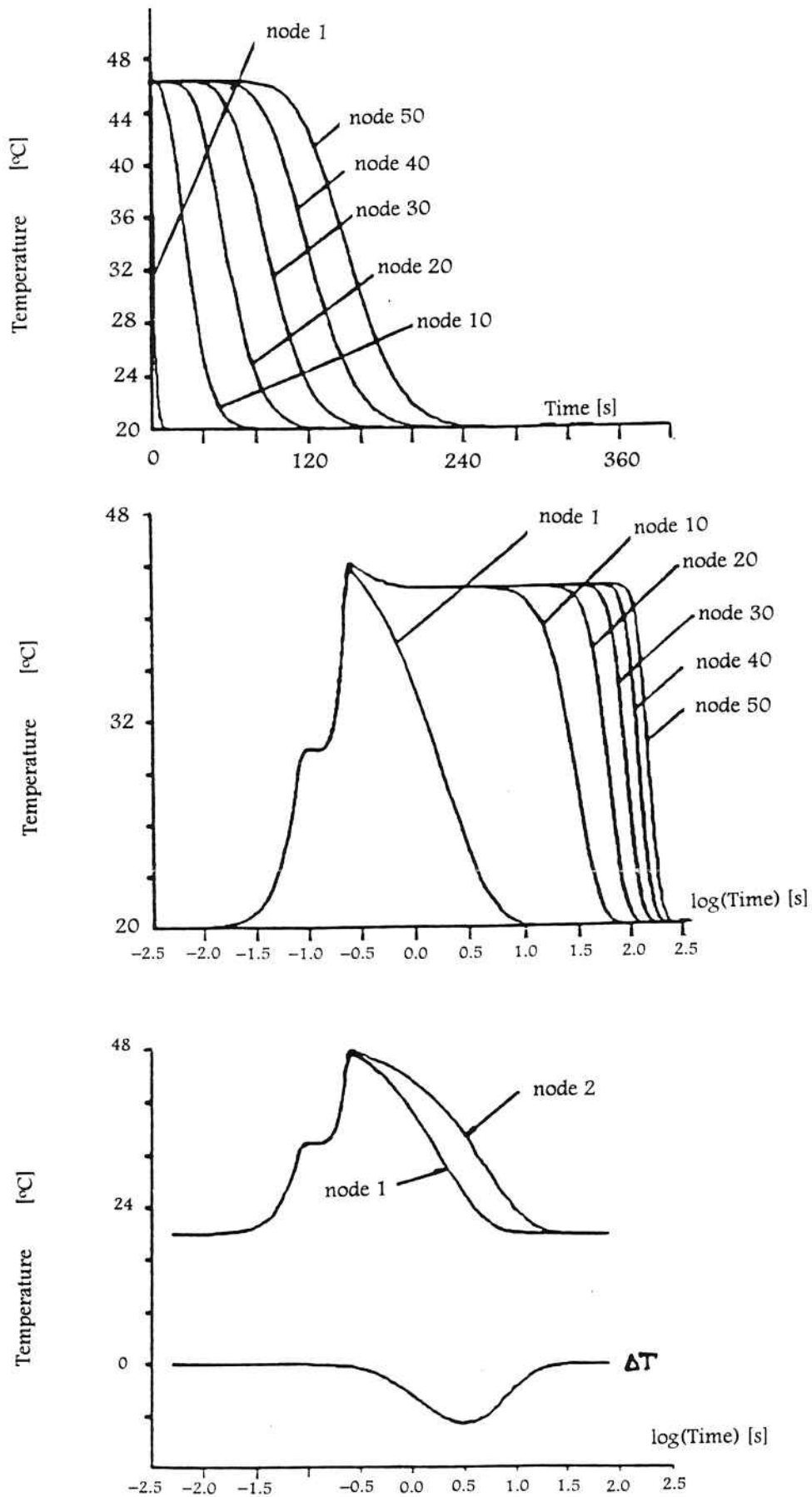


Figure 15 (a) temperature evolution in the initial and final ends and at some equispaced points along the OHS conductor development; (b) the same curves, plotted against the logarithm of time; (c) evolution of the temperature difference between nodes 1 and 2 (worst case).

BOLETINS PUBLICADOS

- 8501 - "Métodos Variacionais Aplicados à Estabilidade dos Taludes e Fundações" - JOSÉ CARLOS DE FIGUEIREDO FERRAZ
- 8502 - "O Processo de Cross Derivado do Método dos Deslocamentos" - JOÃO CYRO ANDRÉ
- 8503 - "Fundações por Bloco" - JOSÉ CARLOS DE FIGUEIREDO FERRAZ
- 8504 - "Investigação Experimental sobre o Valor Limite Wu das Tensões de Cisalhamento no Concreto Estrutural" - PÉRICLES BRASILIENSE FUSCO
- 8505 - "Investigação Experimental sobre o Cisalhamento em Lajes de Concreto Armado" - PERICLES BRASILIENSE FUSCO
- 8506 - "Cálculo das Alterações de Tensão, ao Longo do Tempo, nas Peças de Concreto Protendido: Procedimentos Diretos, Simples, Alternativos ao do CIB" - JOSÉ CARLOS DE FIGUEIREDO FERRAZ
- 8507 - "Elementos de Cálculo Variacional e suas Aplicações nas Estruturas" - JOSÉ CARLOS DE FIGUEIREDO FERRAZ
- 8508 - "Spline Cúbico e suas Aplicações" - CARLOS ALBERTO SOARES
- 8509 - "Correlação Paramétrica Deformatória Flexão Composta, Concreto Armado" - PIETRO CANDREVA
- 8510 - "Lugares Geométricos Notáveis na Flexão Composta - Concreto Armado" - PIETRO CANDREA
- 8511 - "Regiões Deformatórias Notáveis Flexão Composta - Concreto Armado" - PIETRO CANDREVA
- 8512 - "Diagramas Momentos - Curvaturas Flexão Composta Normal - Seções Retangulares Armadura Qualquer nas Barras" - PIETRO CANDREVA
- 8601 - "Alterações, ao Longo do Tempo, dos Estados de Tensão nas Seções de Concreto, Armadas para Diferentes Etapas de Carregamento" - JOSÉ CARLOS DE FIGUEIREDO FERRAZ
- 8602 - "Peças de Concreto Armadas com Barras Protendidas" - JOSÉ CARLOS DE FIGUEIREDO FERRAZ
- 8603 - "A Relaxação do Concreto e a Redistribuição das Tensões nas Peças Armadas" - JOSÉ CARLOS DE FIGUEIREDO FERRAZ
- 8604 - "Análise Não Linear de Trelças Especiais" - PAULO DE MATTOS PIMENTA
- 8605 - "Variação, no Tempo, do Estado de Tensão nas Seções de Concreto Armado" - JOSÉ CARLOS DE FIGUEIREDO FERRAZ
- 8606 - "Evolução ao Longo do Tempo, das Tensões de Cisalhamento nas Vigas de Concreto Protendido" - JOSÉ CARLOS DE FIGUEIREDO FERRAZ
- 8607 - "Cômputo de Fluência por Problemas de Estabilidade" - JOSÉ CARLOS DE FIGUEIREDO FERRAZ
- 8608 - "Erros Usuais Cometidos nas Determinações das Tensões de Cisalhamento nas Peças de Altura Variável" - JOSÉ CARLOS DE FIGUEIREDO FERRAZ
- 8609 - "Contribuição da Fluência do Aço, da Fluência e Retração do Concreto nos Deslocamentos Devidos à Flexão, nas Peças de Concreto Protendido" - JOSÉ CARLOS DE FIGUEIREDO FERRAZ
- 8610 - "Sistema VX-IQB para Processamento de Textos Científicos" - IVAN DE QUEIROZ BARROS
- 8611 - "Análise Não Linear de Pórticos Planos" - PAULO DE MATTOS PIMENTA

- 8612 - "Erros a Serem Evitados no Cálculo de Pórticos, em Particular no dos Edifícios" - JOSÉ CARLOS DE FIGUEIREDO FERRAZ
- 8613 - "Mínima Correctio Methodi Inveniendi Lineas Curvas Elasticii" - PAULO DE MATTOS PIMENTA, CARLOS EDUARDO NIGRO MAZZILLI
- 8614 - "Nova Técnica para Codificações de Procedimentos Envolvendo Matrizes - Avaliação de Desempenho" - IVAN DE QUEIROZ BARROS
- 8615 - "Casos Especiais de Flambagem de Pórticos de Edifícios Altos" - JOSÉ CARLOS DE FIGUEIREDO FERRAZ
- 8616 - "Vigas Protendidas: Alterações das Tensões, das Deformações e dos Deslocamentos ao Longo do Tempo" - JOSÉ CARLOS DE FIGUEIREDO FERRAZ
- 8701 - "Consideração sobre Não-Linearidade Geométrica em Estruturas Reticuladas Planas" - CARLOS EDUARDO NIGRO MAZZILLI
- 8702 - "Consideração da Não-Linearidade Geométrica em Estruturas Laminas Planas" - Parte I - LUIZ ANTONIO CORTESE DIOGO
- 8703 - "Consideração da Não-Linearidade Geométrica em Estruturas Laminas Planas" - Parte II - LUIZ ANTONIO CORTESE DIOGO
- 8704 - "Estado Plano de Tensão (Método dos Resíduos Ponderados e Método dos Elementos Finitos)" - VICTOR M. DE SOUZA LIMA
- 8705 - "Aplicação das Equações de diferenças a um Caso Particular de Estrutura" - JOSÉ CARLOS DE FIGUEIREDO FERRAZ
- 8706 - "Verificação da Estabilidade dos Pilares de Pontes" - JOSÉ CARLOS DE FIGUEIREDO FERRAZ
- 8707 - "Aplicação do Método Variacional ao Cálculo do Empuxo sobre as Paredes de Arrimo" - JOSÉ CARLOS DE FIGUEIREDO FERRAZ
- 8708 - "Análise das Chapas em Regime Elasto - Plástico pelo Método dos Elementos Finitos" - LUIZ ANTONIO CORTESE DIOGO
- 8709 - "Análise das Placas em Regime Elasto-Plástico pelo Método dos Elementos Finitos" - LUIZ ANTONIO CORTESE DIOGO
- 8710 - "A Flambagem de Euler e a "Elástica" Revisitadas: Uma Formulação Unificada para os Cinco Casos Clássicos" - CARLOS EDUARDO NIGRO MAZZILLI
- 8711 - "Laje Protendida e Perdas de Protensão Resultantes da Retração, Fluência do Concreto e do Aço" - JOSÉ CARLOS DE FIGUEIREDO FERRAZ
- 8712 - "O Método dos Elementos Finitos na Solução de Placa, Solicitadas no seu Plano ou Fletidas. Vinculação com o Método de Ritz" - JOSÉ CARLOS DE FIGUEIREDO FERRAZ
- 8713 - "Sobre o Conceito de Corpo Material Linearmente Elástico" - PAULO BOULOS
- 8714 - "Rotações Finitas" - PAULO DE MATTOS PIMENTA
- 8715 - "Efeitos Estruturais de Segunda Ordem nas Treliças" - HENRIQUE DE BRITTO COSTA, YZUMI TAGUTI
- 8716 - "Estudo das Placas: Resíduos Ponderados e Elementos Finitos" - HENRIQUE DE BRITTO COSTA, VICTOR M. DE SOUZA LIMA
- 8717 - "Estacas com Diversos Vínculos de Extremidades Modelo de Winkler. Coeficiente de Reação Lateral do Solo com Distribuição Uniforme" - CARLOS ALBERTO SOARES

Boletins Técnicos -- Títulos Publicados

- 8718 - "Estacas com Diversos Vínculos de Extremidades - Modelo de Winkler. Coeficiente de Reação Lateral do Solo com Distribuição Triangular" - CARLOS ALBERTO SOARES
- 8719 - "Estacas com Diversos Vínculos de Extremidades - Modelo de Winkler. Coeficiente de Reação Lateral do Solo com Distribuição Trapezoidal" - CARLOS ALBERTO SOARES
- 8720 - "Sobre a Matriz de Rigidez Tangente das Barras de Treliças Planas Sujeitas a Rotações Grandes" - LUIZ ANTONIO CORTESE DIOGO
- 8721 - "Um Método Geral para a Redução da Matriz de Rigidez Tangente de Elementos Finitos" - PAULO DE MATTOS PIMENTA
- 8722 - "A Matriz de Rigidez Tangente do Elemento de Pórtico Plano - Teoria de Timoshenko" - PAULO DE MATTOS PIMENTA
- 8801 - "Distribuição Transversal de Carga nas Pontes de Vigas Justapostas" - JOSÉ CARLOS DE FIGUEIREDO FERRAZ
- 8802 - "O Método de Galerkin no Problema das Placas Fletidas - Teoria de Reissner" - HENRIQUE DE BRITTO COSTA
- 8803 - "Um Algoritmo para o Cálculo do Tensão Rotação e do Tensão das Deformações Logarítmicas em Problemas Incrementais" - PAULO DE MATTOS PIMENTA
- 8804 - "Um Algoritmo para a Integração das Tensões na Plasticidade Perfeita" - PAULO DE MATTOS PIMENTA
- 8805 - "Análise das Cascas Cilíndricas em Regime Elasto Plástico pelo Método dos Elementos Finitos" - LUIZ ANTONIO CORTESE DIOGO
- 8806 - "Consideração do Efeito de Membrana nas Placas pelo Método dos Elementos Finitos" - LUIZ ANTONIO CORTESE DIOGO
- 8807 - "Alteração do Estado de Tensão nas Estruturas Hiperestáticas Devida à Fluência do Aço, do Concreto e Retração" - JOSÉ CARLOS DE FIGUEIREDO FERRAZ
- 8808 - "O Método dos Mínimos Quadrados no Exame de alguns Casos de Instabilidade, Computada à Fluência do Material" - JOSÉ CARLOS DE FIGUEIREDO FERRAZ
- 8809 - "A Matriz de Rigidez Tangente do Elemento de Pórtico Espacial" - PAULO DE MATTOS PIMENTA
- 8810 - "Consideração da Fluência do Material da Determinação da Carga Crítica das Barras Mergulhadas em Meio Elástico" - JOSÉ CARLOS DE FIGUEIREDO FERRAZ
- 8811 - "Um Programa para Solução do Problema Generalizado de Autovalores e Autovetores para Matrizes Reais Densas" - PRISCILA GOLDENBERG, REYOLANDO M.L.R.F. BRASIL, MARCIA CIMERMANN
- 8812 - "Pilar de Pontes: Riscos dos Cálculos Correntes" - JOSÉ CARLOS DE FIGUEIREDO FERRAZ
- 8813 - "Sugestes à Norma, em Discussão, sobre Projeto de Estrutura de Concreto Protendido" - JOSÉ CARLOS DE FIGUEIREDO FERRAZ
- 8814 - " Esforços Resistentes do Concreto" - LAURO MODESTO DOS SANTOS
- 8815 - "Tabelas Momento - Curvatura" - LAURO MODESTO DOS SANTOS
- 8816 - "Análise Não-Linear de Arcos" - PAULO DE MATTOS PIMENTA
- 8817 - "Estados Limites das Unies Pregadas de Madeira" - PERICLES BRASILIENSE FUSCO, PEDRO AFONSO DE OLIVEIRA ALMEIDA

- 8818 - "O Emprego da Técnica de Aceleração da Convergência para a Resolução de Problemas Estruturais Através do Método dos Elementos Finitos por Algoritmo do Tipo Resíduo das Tensões" - FRANCISCO BRASILIENSE FUSCO JR., RUBENS AKEL
- 8819 - "Um Critério para o Estabelecimento dos Estimadores de Erro para os Elementos Finitos Adaptativos na Modalidade P" - FRANCISCO BRASILIENSE FUSCO JR. JARBAS A. GUEDES
- 8820 - "Non-Linear Finite-Element Formulation in Dynamic" - CARLOS EDUARDO NIGRO MAZZILLI
- 8821 - "Philosophiae Naturalis Principia Mathematica" de Newton: 300 Anos - JOSÉ CARLOS DE FIGUEIREDO FERRAZ
- 8822 - "A Estabilidade das Fundações Arenosas Estratificadas, Segundo V. V. Sokolovisky" - JOSÉ CARLOS DE FIGUEIREDO FERRAZ
- 8823 - "Flambagem de Estacas Totalmente Enterradas. Solo com Coeficiente de Reação Variável" - CARLOS ALBERTO SOARES
- 8824 - "As Equações de Vlasov e a Estabilidade Espacial das Barras de Seção Delgada" - JOSÉ CARLOS DE FIGUEIREDO FERRAZ
- 8825 - "Um Programa para Solução de Sistemas Lineares de Grande Porte - Aplicação à Engenharia de Estruturas" - PRISCILA GOLDENBERG, REYOLANDO M.L.R.F. BRASIL
- 8826 - "Sobre a Aceleração do Centro Instantâneo de Rotação" - NELSON ACHCAR, PAULO BOULOS
- 8827 - "Esforços Resistentes do Concreto" - LAURO MODESTO DOS SANTOS
- 8828 - "Tabelas Momento-Curvatura" - LAURO MODESTO DOS SANTOS
- 8901 - "A Estimativa da Coesão para o Cálculo da Estabilidade de Aterros e Fundações sobre Argilas Moles" - CARLOS DE SOUSA PINTO
- 8902 - "Trelças Espaciais de Madeira em Regime Viscoelástico sob Não-Linearidade Geométrica" - PAULO DE MATTOS PIMENTA, TAKASHI YOJO
- 8903 - "O Método dos Prismas Equivalentes Aplicado ao Cálculo das Variações de Tensão, ao Longo do Tempo, nas Seções de Concreto" - JOSÉ CARLOS DE FIGUEIREDO FERRAZ
- 8904 - "Efeitos de Laje Concretada Posteriormente sobre Viga Protendida" - JOSÉ CARLOS DE FIGUEIREDO FERRAZ, JOSÉ LOURENÇO BRAGA DE ALMEIDA CASTANHO
- 8905 - "O Cálculo das Grelhas de Pontes pelo Método de Courbon: Uma Hipótese por Demonstrar" - JOSÉ CARLOS DE FIGUEIREDO FERRAZ
- 8906 - "Erosão - Erosão em Área Urbana - Erosão Associada à Construção de Estradas Vicinais" - VERA MARY NINETA COZZOLINO
- 8907 - "Solos Tropicais - Proposta de Classificação Baseada nas Características de Compactação" - VERA MARY NINETA COZZOLINO
- 8908 - "Método Variacional de Cálculo de Construções Estaiadas sob Cargas Dinâmicas" - JOSÉ CARLOS DE FIGUEIREDO FERRAZ
- 8909 - "Métodos Aproximados de Determinação de Frequência de Vibração" - JOSÉ CARLOS DE FIGUEIREDO FERRAZ
- 8910 - "Non-Linear Analysis of Plane Framer I. Quasi-Static Analysis of Plane Framer with Initially Curved Members" - PAULO DE MATTOS PIMENTA

- 8911 - "Non-Linear Analysis of Plane Framer II. Dynamic Analysis of Plane Framer with Initially Curved Members" - PAULO DE MATTOS PIMENTA
- 8912 - "Derivation of Tangent Stiffness Matrices of Simple Finite Elements 1. Straight Bar Elements" - PAULO DE MATTOS PIMENTA
- 8913 - "A Stress Integration Algorithm for the Analysis of Elastic-Plastic Solids by the Finite Element Method I. Small Deformation Analysis" - PAULO DE MATTOS PIMENTA
- 8914 - "A Stress Integration Algorithm For the Analysis of Elastic-Plastic Solids by the Finite Elements Method II. Large Deformation Analysis" - PAULO DE MATTOS PIMENTA
- 8915 - "Flambagem de Estacas Parcialmente Enterradas Solo com Coeficiente de Recalque Constante" - CARLOS ALBERTO SOARES
- 8916 - "Caracterização da Deformabilidade na Elasticidade Linear" - PÉRICLES BRASILIENSE FUSCO
- 8917 - "Um Pacote de Subrotinas Matemáticas para o LMC" - PAULO DE MATTOS PIMENTA, PRISCILA GOLDENBERG
- 8918 - "Relatório de Subrotinas Matemáticas (I)" - PRISCILA GOLDENBERG, PAULO DE MATTOS PIMENTA
- 8919 - "Relatório de Subrotinas Matemáticas (II)" - PAULO DE MATTOS PIMENTA, PRISCILA GOLDENBERG
- 8920 - "Viga Contínua Mista Aço-Concreto, Conectada Elasticamente, sob a Aço da Fluência e Retração" - JOSÉ CARLOS DE FIGUEIREDO FERRAZ
- 8921 - "Relatórios de Subrotinas Matemáticas (III)" - PAULO DE MATTOS PIMENTA, PRISCILA GOLDENBERG
- 8922 - "O Problema da Flexão Plana na Teoria da Elasticidade dos Corpos Não Homogêneos" - JOSÉ CARLOS DE FIGUEIREDO FERRAZ
- 8923 - "Alterações das Tensões de Cisalhamento nas Peças de Concreto Protendido, devidas à Fluência e Retração" - JOSÉ CARLOS DE FIGUEIREDO FERRAZ
- 9001 - "Os Deslocamentos Devidos a Flexão das Vigas Protendidas" - JOSÉ CARLOS DE FIGUEIREDO FERRAZ
- 9002 - "Dinâmica das Estruturas Aporticadas Planas e Comportamento Geometricamente Não Linear" - REYOLANDO M. L. R. F. BRASIL, CARLOS E. N. MAZZILLI
- 9003 - "Teoria de Segunda Ordem das Placas - Estudo da Rigidez Secante" - HENRIQUE DE BRITTO COSTA, VICTOR M. DE SOUZA LIMA
- 9004 - "Influência das Tensões de Cisalhamento na Deformação da Viga sob o Regime Elasto-Plástico" - JOSÉ CARLOS DE FIGUEIREDO FERRAZ
- 9005 - "Ainda a Estabilidade dos Sistemas Elásticos. Aceno Histórico. O Erro de Euler" - JOSÉ CARLOS DE FIGUEIREDO FERRAZ
- 9006 - "A Origem das Funções de Bessel com algumas Aplicações em Problemas Estruturais" - AUGUSTO CARLOS DE VASCONCELOS
- 9007 - "Considerações sobre o Emprego do Teorema dos Trabalhos Virtuais na Resolução de Estruturas Hiperestáticas" - HENRIQUE DE BRITTO COSTA, LUIZ ANTONIO CORTESE DIOGO
- 9008 - "Non-linear Finite-element Formulation in Dynamics II" - CARLOS EDUARDO NIGRO MAZZILLI
- 9009 - "Fatores de Forma e Fatores de Carga Generalizados" - JOSÉ CARLOS DE FIGUEIREDO FERRAZ

- 9010 - "Corpos Hiperelásticos Homogêneos Transversalmente Isotrópicos No Ortotrópicos" - NELSON ACHCAR
- 9011 - "Análise das Cascas de Revolução em Regime Elasto Plástico pelo Método dos Elementos Finitos" - JOSÉ MARQUES FILHO, LUIZ ANTONIO CORTESE DIOGO
- 9012 - "O Algoritmo de Mínimo Grau para Reordenação e Solução de Sistemas Lineares Esparsos" - PRISCILA GOLDENBERG, REYOLANDO M. L. R. F. BRASIL, SÉRGIO PINHEIRO
- 9101 - "Consideração da Não-Linearidade Física e da Não-Linearidade Geométrica na Análise das Placas pelo Método dos Elementos Finitos - Parte 1" - LUIZ ANTONIO CORTESE DIOGO
- 9102 - "Introdução ao Estudo dos Pórticos Esbeltos - Matriz de Rigidez Secante" - HENRIQUE DE BRITTO COSTA, ALFONSO PAPPALARDO JR.
- 9103 - "Cálculo de Estruturas Sujeitas a Terremotos" - HENRIQUE DE BRITTO COSTA, SELMA H. SHIMURA
- 9104 - "Análise Não - Linear de Pórticos Espaciais - Parte I: Teoria e Método dos Elementos Finitos" - PAULO M. PIMENTA, TAKASHI YOJO
- 9105 - "Flambagem de Edifícios Altos" - JOSÉ CARLOS DE FIGUEIREDO FERRAZ
- 9106 - "Programas de Microcomputador para Análise Dinâmica de Estruturas nos Domínios do Tempo e da Freqüência" - REYOLANDO M.L.R. DA F. BRASIL
- 9107 - "Variação nas Peças Protendidas" - JOSÉ CARLOS DE FIGUEIREDO FERRAZ
- 9108 - "Análise das Placas Sujeitas a Grandes Rotações Mediante o Uso do Método dos Elementos Finitos" - LUIZ ANTONIO CORTESE DIOGO
- 9109 - "Consideração Tópica sobre o Código Modelo 1990 do CEB-FIP" - JOSÉ CARLOS DE FIGUEIREDO FERRAZ
- 9110 - "Materiais Compatíveis com as Barras Cujas Secções Normais Permanecem Planas" - NELSON ACHCAR
- 9111 - "Dinâmica das Placas: Elementos Finitos via Resíduos Ponderados" - HENRIQUE DE BRITTO COSTA, FLAVIO JOSÉ GARZERI, REYOLANDO M. L. R. FONSECA BRASIL
- 9112 - "Estabilidade do Equilíbrio dos Sistemas no Campo Conservativo de Forças" - JOSÉ CARLOS DE FIGUEIREDO FERRAZ
- 9113 - "Sobre a Estabilidade Elástica de Arcos Abatidos" - REYOLANDO M. L. R. FONSECA BRASIL, VICTOR M. DE SOUZA LIMA
- 9114 - "Considerações Teóricas sobre o Adensamento Secundário" - HELOISA HELENA SILVA GONÇALVES
- 9115 - "Teoria de Vlassov sobre Barras, Placas e Cascas, de Parede Fina, Protendidas" - JOSÉ CARLOS DE FIGUEIREDO FERRAZ
- 9201 - "Consideração da Não-Linearidade Física e da Não-Linearidade Geométrica na Análise das Placas pelo Método dos Elementos Finitos - Parte II" - LUIZ ANTONIO CORTESE DIOGO
- 9202 - "Sobre a Interpretação de Provas de Carga em Estacas Considerando as Cargas Residuais de Ponta e a Reversão do Atrito Lateral" - FAIÇAL MASSAD
- 9203 - "Um Programa para Análise Limite de Pórticos Planos em Regime Elasto-Plástico" - REYOLANDO M.L.R. DA FONSECA BRASIL
- 9204 - "Equação Constitutiva das Barras Hiperelásticas Transversalmente Isotrópicas" - NELSON ACHCAR
- 9205 - "Análise Não-Linear de Pórticos Espaciais de Madeira" - PAULO DE MATTOS PIMENTA, TAKASHI YOJO

- 9206 - "Perda de Estabilidade à Tração" - JOSÉ CARLOS DE FIGUEIREDO FERRAZ
- 9207 - "Teoria de Segunda Ordem das Placas - Estudo da Rigidez Tangente" - HENRIQUE DE BRITTO COSTA, VICTOR M. DE SOUZA LIMA
- 9208 - "Vibrações Não-Lineares de Placas" - HENRIQUE DE BRITTO COSTA, REYOLANDO M. L. R. DA FONSECA BRASIL, PAULO SHIGUEME IDE
- 9209 - "Variedades Vinculadas Reduzidas" - PAULO BOULOS, NELSON ACHCAR,
- 9210 - "Estudo da Perda de Estabilidade Segundo Critérios Dinâmicos" - JOSÉ CARLOS DE FIGUEIREDO FERRAZ
- 9211 - "Programas de Microcomputador para Análise Dinâmica de Estruturas - Parte II - Vários Graus de Liberdade" - REYOLANDO M. L. R. DA FONSECA BRASIL
- 9212 - "Otimização da Deposição de Rejeitos" - LUIZ GUILHERME F. S. DE MELLO
- 9213 - "Andros - a Finite Element Program From Nonlinear Dynamics" - CARLOS EDUARDO NIGRO MAZZILLI, REYOLANDO M. L. R. DA FONSECA BRASIL
- 9214 - "Considerações sobre o Cálculo Dinâmico de Estruturas Usando Transformadas de Fourier" - ALFREDO PINTO DA CONCEIÇÃO NETO, VICTOR M. DE SOUZA LIMA
- 9215 - "Placas Delgadas" - ALFONSO PAPPALARDO JUNIOR, HENRIQUE DE BRITTO COSTA
- 9216 - "Excitação Paramétrica em Sistemas com um Grau de Liberdade" - MARIO EDUARDO SENATORE SOARES, CARLOS EDUARDO NIGRO MAZZILLI
- 9301 - "PEFMAT - Relatórios de Subrotinas Matemáticas - Parte IV" - PRISCILA GOLDENBERG, PAULO DE MATTOS PIMENTA, MARCIA CIMERMAN
- 9302 - "Vibrações de Pórticos com Vigas de Rigidez Infinita" - JOSÉ CARLOS DE FIGUEIREDO FERRAZ
- 9303 - "Direct Along - Wind Dynamic Analysis of Tall Structures" - MARIO FRANCO
- 9304 - "Comportamento Pós-Crítico de Barra Delgada Protendida" - JOSÉ CARLOS DE FIGUEIREDO FERRAZ
- 9305 - "Os Polinômios Trigonométricos na Solução de Problemas de Vibração Mecânica" - JOSÉ CARLOS DE FIGUEIREDO FERRAZ
- 9306 - "Linhas de Influência Dinâmicas para Deslocamentos, Momentos Fletores e Forças Cortantes nas Vigas Simples" - JOSÉ CARLOS DE FIGUEIREDO FERRAZ
- 9307 - "O Modelo Clam-Clay Revisto" - JOSÉ JORGE NADER
- 9308 - "Patologia da Concepção Estrutural: Danos por Efeitos de Segunda Ordem em Edifícios Altos, um Exemplo" - PÉRICLES BRASILIENSE FUSCO
- 9309 - "Vibração de Sistemas Não Lineares: Método de Aproximações Sucessivas" - JOSÉ CARLOS DE FIGUEIREDO FERRAZ
- 9310 - "Normalização dos Símbolos Gráficos para Projetos de Estruturas de Madeira" - PÉRICLES BRASILIENSE FUSCO
- 9311 - "Ensaio de Adensamento" - HELOISA HELENA SILVA GONÇALVES
- 9312 - "Comentários sobre a Normalização das Ações e Segurança nas Estruturas" - PÉRICLES BRASILIENSE FUSCO

- 9313 - "Introdução à Análise Dinâmica de Estruturas por Meio de Elementos Finitos - Parte I - Galerkin e Elementos Finitos" - HENRIQUE DE BRITTO COSTA, SELMA HISSAE SHIMURA
- 9314 - "Vibrações Aleatórias na Dinâmica de Estruturas" - REYOLANDO M. L. R. F. BRASIL
- 9315 - "Determinação da Equação para Cálculo do Momento Crítico à Flambagem Lateral" - VALDIR PIGNATTA E SILVA, LUIZ ANTONIO CORTESE DIOGO
- 9316 - "Efeito dos Sismos nas Estruturas Aporticadas" - JOSÉ CARLOS DE FIGUEIREDO FERRAZ
- 9317 - "As Estruturas Aporticadas com Vigas de Rigidez Infinita, Submetidas ao Sismo" - JOSÉ CARLOS DE FIGUEIREDO FERRAZ
- 9318 - "Uma Proposta de Normalização das Resistências da Madeira Estrutural" - PÉRICLES BRASILIENSE FUSCO
- 9319 - "Resistência dos Materiais Anisotrópicos" - PÉRICLES BRASILIENSE FUSCO
- 9401 - "Soluções Analíticas para a Deformação do Material Elasto - Plástico Cam - Clay úteis na Interpretação de Ensaio Triaxiais com Diferentes Trajetórias de Tensão" - JOSÉ JORGE NADER
- 9402 - "Introdução à Fotoelasticidade por Reflexão" - PEDRO AFONSO DE OLIVEIRA ALMEIDA, FRANCISCO ROURE FERNANDEZ, FREDERIC MARINON CARVAJAL
- 9403 - "Numerical Conditioning in Structural Solutions: a Proposal for a new Condition Number" - HENRIQUE LINDENBERG NETO
- 9404 - "A Esbeltez Estrutural e sua Influência nas Frequências de Vibrações" - JOSÉ CARLOS DE FIGUEIREDO FERRAZ
- 9405 - "Determinação do Momento Crítico à Flambagem Lateral de Viabilizadas de Aço" - VALDIR PIGNATTA E SILVA, LUIZ ANTONIO CORTESE DIOGO
- 9406 - "Uma Análise dos Parâmetros de Ensaio Utilizados para Cálculo de Recalques por Adensamento" - HELOISA HELENA SILVA GONÇALVES
- 9407 - "Programação Matemática Aplicada à Análise Limite de Estruturas" I - PAULO DE MATTOS PIMENTA, PRISCILA GOLDENBERG, ERNESTO COUTINHO COLLA
- 9408 - "Programação Matemática Aplicada à Análise Limite de Estruturas II" - PAULO DE MATTOS PIMENTA, PRISCILA GOLDENBERG, ERNESTO COUTINHO COLLA
- 9409 - "Formulação de um Elemento Finito de Cabo Incorporando o Efeito do Atrito" - RUY M. PAULETTI, PAULO M. PIMENTA
- 9410 - "A Descrição do Domínio para o Projeto por Elementos Finitos" - JOSÉ ANTONIO LEROSA SIQUEIRA, JOO CYRO ANDRÉ
- 9411 - "O Método dos Elementos Finitos Aplicado a uma Formulação Mista da Teoria das Placas" - MYRIAM RENATA DIAS FERREIRA, HENRIQUE DE BRITTO COSTA
- 9412 - "Problemas Envolvendo Ponto, Reta e Plano, Tratados Vetorialmente" - JOSÉ CARLOS DE FIGUEIREDO FERRAZ
- 9413 - "Auto - Sincronização de Motores Não - Ideais Apoiados em Estruturas Elásticas" - PETRUS GORGONIO BULHES DA NBREGA, CARLOS EDUARDO NIGRO MAZZILLI
- 9501 - "Global and Local Instability of Concrete Tall Buildings" - M. FRANCO
- 9502 - "Um Elemento Finito Giroscópio" - MARCELO GONZALES BERGWELER, CARLOS EDUARDO NIGRO MAZZILLI

- 9503 - "Teoria da Segunda Ordem das Placas - Uma Formulação Mista" - SELMA HISSAE SHIMURA, HENRIQUE DE BRITTO COSTA
- 9504 - "Modelagem de Corpos Sólidos: Topologia e Operadores de Euler" - BENEDITO ROQUE DE GUIMARÃES ARANTES JUNIOR, JOÃO CYRO ANDRÉ, JOSÉ ANTONIO LEROSA DE SIQUEIRA
- 9505 - "Investigação Experimental em Laje de Concreto Armado Apoiada em Vigas Flexíveis" - ANTONIO RUBENS PORTUGAL MAZZILLI
- 9506 - "Influência da Flexibilidade das Vigas e das Lajes nos Esforços das Estruturas de Concreto Armado" - ANTONIO RUBENS PORTUGAL MAZZILLI
- 9507 - "A Calibração da Segurança na Nova Norma de Projeto de Estruturas de Madeira" - PÉRICLES BRASILIENSE FUSCO
- 9508 - "Método de Ensaio de Punção Excêntrica em Placa de Concreto" - FÁBIO ARMANDO BOTELHO CORDOVID, PÉRICLES BRASILIENSE FUSCO
- 9509 - "Ensaio de Placas de Concreto Armado - Punção Excêntrica" - FÁBIO ARMANDO BOTELHO CORDOVID, PÉRICLES BRASILIENSE FUSCO
- 9510 - "Armadura de Cisalhamento para Punção em Placas de Concreto" - FÁBIO ARMANDO BOTELHO CORDOVID, PÉRICLES BRASILIENSE FUSCO
- 9511 - "Aspectos Normativos sobre Punção em Placas de Concreto Armado" - FÁBIO ARMANDO BOTELHO CORDOVID, PÉRICLES BRASILIENSE FUSCO
- 9512 - "Alternativas de Representação da Protensão, no Projeto de Estruturas de Concreto" - KALIL J. SKAF, FERNADO R. STUCCHI
- 9513 - "Aplicações do Lagrangeano Aumentado em Otimização Estrutural" - PAULO DE MATTOS PIMENTA, PRISCILA GOLDENBERG, REYOLANDO BRASIL
- 9514 - "Análise Linear da Estabilidade de Treliças Utilizando o Método de Lanczos" - CÉLIA REGINA MORETTI MEIRELLES, PAULO DE MATTOS PIMENTA
- 9515 - "Análise Dinâmica de Pórticos Planos sob Ação de Carregamentos Transientes Considerando Formação de Rótulas Plásticas" - REYOLANDO M. L. R. F. BRASIL, CESAR FERNANDES JUNIOR
- 9516 - "A Engenharia da Fusão Termonuclear Controlada. Sua História e seu Futuro" - RUY MARCELO DE OLIVEIRA PAULETTI, VICTOR MANOEL DE SOUZA LIMA
- 9517 - "Considerações sobre o Emprego do Teorema dos Trabalhos Virtuais na Resolução de Estruturas Hiperestáticas: - Pórticos" - HENRIQUE DE BRITTO COSTA, LUIZ ANTONIO CORTESE DIOGO
- 9518 - "Flambagem Lateral de Vigas de Madeira" - VALDIR PIGNATTA E SILVA
- 9519 - "Diagramas Tensão-Deformação dos Aços Estruturais Submetidos a Altas Temperaturas" - VALDIR PIGNATTA E SILVA, PAULO DE MATTOS PIMENTA
- 9520 - "Uma Aplicação da Teoria Constitutiva dos Materiais Elásticos-Lineares Sujeitos a Vínculos Internos: Dedução Exata da Equação de Lagrange para Placas Finas" - JOÃO MAURÍCIO SAPIENZA, NELSON ACHCAR
- 9521 - "Conceitos Básicos sobre Geração Automática de Malha" - JOSÉ FERNANDO MANTOVANI MICALI, JOÃO CYRO ANDRÉ
- 9522 - "Equações Constitutivas do Concreto Baseadas na Mecânica do Dano Contínuo" - FLÁVIO LUIZ DE S. BUSSAMRA, PAULO DE M. PIMENTA

[The page contains extremely faint, illegible text, likely bleed-through from the reverse side of the document. The text is too light to transcribe accurately.]